

The Effects of Hypoxic Preconditioning on the Oxygenation and Metabolic Profile of Neuroblastoma – Yousef Al-Mutawa



UNIVERSITY OF
LIVERPOOL

The Effects of Hypoxic Preconditioning on the Oxygenation and Metabolic Profile of Neuroblastoma

Thesis submitted in accordance with the requirements of the University of Liverpool for the Degree of Master of Philosophy by:

Yousef Al-Mutawa

November 2017

The Effects of Hypoxic Preconditioning on the Oxygenation and Metabolic Profile of Neuroblastoma – Yousef Al-Mutawa

Table of Contents

| | |
|---|-----------|
| Acknowledgement | 4 |
| Abstract | 5 |
| 1. Introduction | 6 |
| <i>1.1 Neuroblastoma – A Clinical Perspective</i> | 6 |
| 1.1.1 Embryology & Genetics | 6 |
| 1.1.2 Pathology & Staging | 7 |
| 1.1.3 Screening, Presentation, and Diagnosis | 11 |
| 1.1.3.1 Regression | 11 |
| 1.1.3.2 Screening | 11 |
| 1.1.3.3 Presentation | 11 |
| 1.1.4 Treatment | 12 |
| <i>1.2 Neuroblastoma – A Biological Perspective</i> | 13 |
| 1.2.1 Cancer Cell Metabolism | 13 |
| 1.2.2 Metabolomics | 14 |
| 1.2.3 Hypoxia | 15 |
| 1.2.3.1 Causes | 16 |
| 1.2.3.2 Hypoxia and Neuroblastoma | 18 |
| 1.2.4 Chick Embryo CAM Model | 18 |
| 1.2.4.1 Introducing the model | 18 |
| 1.2.4.2 Suitability for Neuroblastoma Research | 19 |
| 1.2.4.3 Limitations | 19 |
| 1.2.5 SK-N-AS Cells | 19 |
| <i>1.3 Hypothesis</i> | 20 |
| <i>1.4 Project Aim</i> | 20 |
| 2. Methods | 20 |
| 2.1 Egg incubation | 21 |
| 2.2 Windowing | 21 |
| 2.3 Chorioallantoic implantation (Embryonic day 7) | 24 |
| 2.4 In-vivo Oxygen Measurement | 25 |
| 2.5 Tumour Extraction | 27 |
| 2.5.1 Tumour snap freezing (for NMR) | 27 |
| 2.5.2 Tumours fixation and staining (for immunostaining) | 27 |
| 2.6 Tumour Slicing for Imaging | 28 |
| 2.7 Cell culture | 29 |
| 2.7.1 Cell Collection and Freezing prior to Lipid Extraction for NMR | 30 |
| 2.7.2 Calculating cell number | 30 |
| 2.7.3 Hypoxic Incubation | 30 |
| 2.8 Immunofluorescence and Imaging | 30 |
| 2.9 Metabolomic Analysis | 32 |
| 2.9.1 Acetyl-Nitrile H ₂ O (AcN-H ₂ O) Tumour extraction | 32 |
| 2.9.2 Acetyl-Nitrile H ₂ O (AcN-H ₂ O) Cell pellet extraction | 32 |
| 2.9.3 Sample Preparation | 32 |
| | 2 |

The Effects of Hypoxic Preconditioning on the Oxygenation and Metabolic Profile of Neuroblastoma – Yousef Al-Mutawa

| | |
|---|-----------|
| 2.9.4 NMR Acquisition | 33 |
| 2.9.5 Spectral Processing | 33 |
| 2.10 Statistical Analysis | 33 |
| 2.10.1 Principal Component Analysis (PCA) and Discriminant Analysis of Principal Components (DAPC) | 33 |
| 3. Results | 35 |
| 3.1 Hypoxic Preconditioning of cells does not significantly affect oxygen tension of tumours | 35 |
| 3.1.1 Differences in Tumour Oxygenation | 35 |
| 3.1.2 Oxygen Fluctuation is not affected by hypoxic preconditioning | 37 |
| 3.1.3 Fluctuation does not increase with longer measurements | 39 |
| 3.2 Metabolomic analysis of cell and tumour samples | 40 |
| 3.2.1 Principal Component Analysis | 40 |
| 3.2.2 Discriminant analysis of Principal components (DAPC) | 42 |
| 3.2.3 Discriminant Analysis of specific metabolites to distinguish Hypoxia from Normoxia | 45 |
| 3.2.3.1 Contrasting metabolite regulation between neuroblastoma cells and tumours formed on the CAM | 49 |
| 4. Discussion | 52 |
| 4.1 Tumour Oxygenation | 52 |
| 4.1.1 The Effect of Hypoxic Preconditioning | 52 |
| 4.1.2 Oxygen Fluctuation | 53 |
| 4.1.3 Limitations of oxygen measurements | 54 |
| 4.2 Metabolomics | 54 |
| 4.2.1 Principal component analysis (PCA) | 54 |
| 4.2.2 Heatmap | 55 |
| 5. Conclusion | 58 |
| 6. Appendix | 59 |
| 7. References | 62 |

Acknowledgement

I would like to express my immense gratitude to my supervisors Professor Paul Losty and Dr. Violaine See who have welcomed me into their exceptional team and provided me with the continuous support and guidance necessary to succeed in this project. It was a massive pleasure and honour to have initiated my career working with them. During this time, I have participated in clinical and scientific conferences with abstract submissions, poster presentations, and a short talk. We are also in the process of publishing our research. I wish to thank you again for these valuable opportunities.

It was a privilege to work alongside Dr. Marie Phelan whose contributions and expertise were central to the success of this work. I wish to thank Dr. Phelan and Rudi Grosman for their assistance and advice throughout this project.

I am particularly grateful to Dr. Anne Herrmann who has been my mentor since day one in every aspect of this project with her kind manners and exemplary teaching skills. I have so often turned to Anne for her advice and astute analysis at times where the work was at a complicated stage and we would have a troubleshooting session that would always clear the way forward.

I would like to thank Dr. Diana Moss for her generous support in her lab and for taking care of the logistics involved in our chick embryo experimentation. I would like to extend my thanks to everyone involved in the Liverpool Centre for Cell Imaging, particularly Dr. David Mason, and to all my colleagues in Lab B at the Institute of Integrative Biology.

I wish to extend my gratitude to the Ministry of Higher Education (Kuwait), in particular to Professor Nouriya Al-Awadhi and Mrs. Roula Al-Omar, who believed in me and supported my application for postgraduate studies. I wish to thank the Cultural Attache at the Kuwait Cultural Office, Mrs. Wafaa Al-Kharji, and all the academic and administrative staff at the Cultural Office for their ongoing support throughout my studies.

Finally, I am forever indebted to my family for their endless stream of encouragement and support. To my mother, Afraa, who lifts my spirits and ignites my determination. To my father, Khalid, who is never short of encouraging words and praise. To my wife, Hayfaa, whose kind patience and fervent support maintained the smooth sailing of this project. To my sister, Munirah, whose involvement in my studies were paramount to my success. I would like to thank them all and thank everyone who was part of my journey and whose names would fill an entire dissertation. I am grateful to them all.

Abstract

Despite neuroblastoma being the most common extracranial solid malignancy in children, it presents a significantly atypical challenge to clinicians and researchers due to its complex biological interplay and heterogeneous behaviour. Hypoxia, which is a lack of oxygenation, has been implicated as a significant factor leading to metastasis, treatment resistance and poor prognosis in many cancers, including neuroblastoma. Whilst our lab has previously demonstrated that hypoxic pre-conditioning of neuroblastoma cells directly triggers neuroblastoma tumour metastasis, it is not known how such preconditioning affects the tumour's oxygenation itself and how it alters the tumour's metabolism.

We initially measured intratumoural oxygenation, using a fibre-optic oxygen sensor, in tumours originating from neuroblastoma cells and growing on the chorioallantoic membrane (CAM) of a chick embryo model. We investigated the effects of hypoxia preconditioning of the cells on the actual oxygen levels within the tumour. We further investigated, using Nuclear Magnetic Resonance (NMR), the effects of hypoxic preconditioning on the metabolic profile of neuroblastoma tumours.

We demonstrated that hypoxic preconditioning had only a minor effect on intratumoural oxygenation values, yet it had a significant measurable influence on the metabolic profile of the tumours.

In particular, 13 metabolites showed a consistent response to hypoxia, with 9 being decreased and 4 being increased in the hypoxic sets across cells and tumour, thus illustrating the lasting effects of hypoxic preconditioning on the tumour metabolome.

1. Introduction

1.1 Neuroblastoma – A Clinical Perspective:

Neuroblastoma is a paediatric cancer of remarkable heterogeneity that exhibits an equally perplexing biological and clinical behaviour ranging from asymptomatic spontaneous regression to an aggressive metastatic treatment-resistant disease. It is the most common extracranial solid tumour in childhood and is accountable for almost 8% of all paediatric malignancies and 11-15% of paediatric oncology fatalities with an overall survival rate at around approximately 40% (1-3). Neuroblastoma arises as a consequence of multiple genetic and environmental insults during the early stages of neural crest development leading to malignant cellular differentiation (4, 5).

1.1.1 Embryology & Genetics:

A series of cellular signalling events termed the epithelial-to-mesenchymal transition (EMT) leads to migration, specification, and differentiation of cells that subsequently develop the basis of embryological formation (4, 6). Cells originating from the ectoderm develop to form a significant proportion of what is collectively known as the nervous system that includes the brain, spinal cord, sympathetic chain, cardiac and enteric ganglia, autonomic network, in addition to the adrenal glands (4, 7-9). A multitude of genetic and epigenetic factors play a role during neural crest development and EMT to contribute to the development of neuroblastoma (4). However, an individual genetic or epigenetic factor has not been implicated as the sole trigger for neuroblastoma development (10). Although not all the players have been identified, several have been implicated as oncogenic drivers in neuroblastoma. Chromosomal deletions are detected in approximately 50% of neuroblastoma cases and are associated with a poor prognosis (11-14). The chromosomal deletions most commonly detected in chromosomes 1p, 11q, and 14q in addition to chromosome 17q gain and MYCN gene amplification demonstrate the biological interplay resulting in the heterogeneity of neuroblastoma presentation and prognosis (4, 10, 15-17). The genetic amplification of the MYCN oncogene in approximately 20-25% of neuroblastoma cases is considered as a trigger of metastatic potential and a poor prognostic marker (17-20). Other alterations associated with cellular development arrest and neuroblastoma

The Effects of Hypoxic Preconditioning on the Oxygenation and Metabolic Profile of Neuroblastoma – Yousef Al-Mutawa

tumourigenesis include anaplastic lymphoma kinase (ALK) gene mutations, neurotrophic growth factor (NGF) expression, and changes in DNA content (4, 21).

Evidently, this interplay of multiple factors during the early stages of embryogenesis complicates the identification of a primary pathway for the pathogenesis of neuroblastoma and demonstrates the spectrum of neuroblastoma heterogeneity.

1.1.2 Pathology & Staging:

The unique complexity of neuroblastoma is highlighted by the spectrum of the malignancy that ranges from asymptomatic spontaneous regression to a fatal aggressive metastatic disease. This heterogeneity is reflected in all aspects of the disease including the staging and classification systems, broad range of clinical presentations and behaviour, multimodal treatment approaches, selective therapeutic responsiveness, and range of prognostic factors. Neuroblastoma lies within a spectrum of neuroblastic tumours classified by the International Neuroblastoma Pathology Classification (INPC) based on the proportion of neural derived cells and Schwannian stroma cells (22). Ganglioneuroma is the most differentiated subtype and is dominant in schwannian stroma followed by ganglioneuroblastoma (22). The least differentiated subtype, neuroblastoma, is poor in schwannian stroma and consequently the most aggressive neuroblastic tumour (22).

Conventionally, the International Neuroblastoma Staging System (INSS) has been widely adopted since its development in 1986 (23). Tumour staging relies mainly on a post-surgical assessment of the tumour as outlined in table 1 below adapted from Brodeur and Pritchard et al., 1993 (24).

INTERNATIONAL NEUROBLASTOMA STAGING SYSTEM (POST-SURGICAL STAGING)

| Stage | Description |
|-----------|--|
| 1 | Localised tumour confined to the area of origin; complete gross excision with or without microscopic residual disease; identifiable ipsilateral and contralateral lymph nodes microscopically negative. |
| 2a | Unilateral tumour with incomplete gross excision; identifiable ipsilateral and contralateral lymph nodes microscopically negative. |
| 2b | Unilateral tumour with incomplete gross excision with positive ipsilateral regional lymph nodes; identifiable contralateral lymph nodes microscopically negative. |
| 3 | Tumour infiltrating across the midline with or without regional lymph node involvement; or unilateral tumour with contralateral regional lymph node involvement; or midline tumour with bilateral regional lymph node involvement. |
| 4 | Dissemination of tumour to bone, bone marrow, liver, distant lymph nodes, and/or other organs except as defined for stage 4S |
| 4s | Localised primary tumour –as defined for stages 1 or 2- with dissemination limited to liver, skin, and/or <10% of bone marrow. Age <1 year at diagnosis. |

Table 1. The International Neuroblastoma Staging System

This classification system developed in 1986 has been widely accepted and adopted as a staging tool for neuroblastoma. This tool stages neuroblastoma from a pre and post-surgical perspective and precedes the International Neuroblastoma Risk Group Staging System (INRGSS).

Adapted from Brodeur and Pritchard et al., 1993 (24)

In parallel with ongoing discoveries around the biological complexity of neuroblastoma over the past two decades, the necessity to develop a staging system independent of surgical intervention became apparent. This culminated in the introduction of the International Neuroblastoma Risk Group Staging System (INRGSS) in 2009 (25, 26). The INRGSS staging is

The Effects of Hypoxic Preconditioning on the Oxygenation and Metabolic Profile of Neuroblastoma – Yousef Al-Mutawa

dependent on pre-surgical imaging assessment with 2 stages for localised disease (L1 and L2) and 2 stages, M and MS, for metastatic disease (Table 2).

International Neuroblastoma Risk Group Staging System (INRGSS)

| Stage | Definition |
|-----------|---|
| L1 | Tumour localised and confined within 1 body compartment; no vital structure involvement. |
| L2 | Locoregional tumour + 1 or more image defined risk factors (IDRF) |
| M | Metastatic Disease unless stage MS |
| MS | Metastatic Disease in children <18 months old. Metastasis confined to skin and/or liver and/or bone marrow. |

Table 2. The International Neuroblastoma Risk Group Staging System

The INRGSS was developed to implement an imaging based staging system independent of, and prior to, surgical intervention.

Adapted from: Monclair et al. 2009 (25)

Additionally, there are 20 image-defined risk factors (IDRFs) that complement staging in the INRGSS and are identified in table 3 below as adapted from Monclair et al., 2009 (25).

Image Defined Risk Factors in Neuroblastoma

| Region: | Tumour: |
|--|--|
| Ipsilateral Tumour within 2 Body Compartments | Neck-chest, chest-abdomen, abdomen-pelvis |
| Neck | Encasing carotid and/or vertebral artery and/or internal jugular vein, Extending to base of skull Compressing the trachea |
| Cervicothoracic Junction | Encasing brachial plexus roots, and/or subclavian vessels, and/or vertebral/carotid artery Compressing the trachea |
| Thorax | Encasing aorta and/or major branches Compressing the trachea and/or principal bronchi, Lower mediastinal tumour, infiltrates the costo-vertebral junction between T9 and T12. |
| Thoraco-Abdominal | Encasing the aorta and/or vena cava |
| Abdomen/Pelvis | Infiltrating the porta hepatis and/or the hepatoduodenal ligament Encasing branches of the superior mesenteric artery at the mesenteric root, Encasing the origin of the coeliac axis, and/or of the superior mesenteric artery Invading one or both renal pedicles Encasing the aorta and/or vena cava, Encasing the iliac vessels Pelvic tumour crossing the sciatic notch |
| Organ and Structure Infiltration | Pericardium, diaphragm, kidney, liver, duodeno-pancreatic block and mesentery |

Table 3. The Image Defined Risk Factors in Neuroblastoma

The INRGSS identifies 20 image-defined risk factors (IDRF) to complement the staging system of neuroblastoma.

Adapted from: Monclair et al. 2009 (25)

The Effects of Hypoxic Preconditioning on the Oxygenation and Metabolic Profile of Neuroblastoma – Yousef Al-Mutawa

1.1.3 Screening, Presentation, and Diagnosis:

1.1.3.1 Regression

Spontaneous tumour regression is an intriguing feature of neuroblastoma. Although not exclusive to neuroblastoma, spontaneous regression in neuroblastoma is the most common across malignancies such as renal, malignant melanoma, choriocarcinoma, and lymphoid carcinoma (27-30). This enigmatic tendency illustrates the spectra of heterogeneity in neuroblastoma from spontaneous regression to therapeutic resistance and mortality. Current understanding of the biological and genetic mechanisms responsible for this tendency are limited, however, mass screening programmes in Japan, Austria, Germany, and Canada have shed light on this intriguing characteristic (31-36).

1.1.3.2 Screening:

Mass screening of infants in Japan tested urine for Vanillylmandelic acid (VMA) and Homovanillic Acid (HVA) from 1973 until 1989 (32). As a result, there was a noticeable increase in neuroblastoma detection with an insignificant decrease in the overall mortality rates (31, 32, 35). Cases that would spontaneously regress were almost as equal as cases that would have eventually been detected clinically. Consequently, all the neuroblastoma screening programmes have been suspended as they have not achieved their intended targets of significantly decreasing mortality rates (30, 31). They have, however, contributed valuable insight to scientists and clinicians seeking new ways to approach and investigate neuroblastoma.

1.1.3.3 Presentation:

As neuroblastoma arises from the neural crest precursor cells, the resulting tumour may arise from any site of the sympathetic chain, adrenal glands, or the central and autonomous nervous systems. Tumours develop in the adrenal glands, abdomen, thoracic cavity, neck, and the pelvic sympathetic ganglia. These tumours may metastasise to the liver, skin, lymph nodes, bone, bone marrow, dura, eye orbits, and skin (24, 37, 38). The incidence of metastasis at diagnosis in a series of 648 children with stage 4 and 4s neuroblastoma showed 70.5% in bone marrow, 55.7% in bone, 30.9% in lymph nodes, 29.6% in liver, 18.2% in head, neck and orbits, 3.3% in lungs, and 0.6% in the CNS (37).

The Effects of Hypoxic Preconditioning on the Oxygenation and Metabolic Profile of Neuroblastoma – Yousef Al-Mutawa

Presentation can be as variable as the sites of neuroblastoma formation and ranges from asymptomatic to systemic illness. Intra-abdominal tumours usually present with distension, abdominal pain, and weight loss (39). Tumours arising from the thorax cause mechanical obstruction and respiratory compromise and present with dyspnoea, stridor, cough, tracheal compression or deviation (39, 40). Horner's syndrome, a triad of ptosis, miosis, and anhidrosis, is associated with high thoracic tumours in neuroblastoma (39, 40). A paraspinal tumour leads to loss of anal sphincter control and urinary incontinence which may require an emergency intervention (39). Periorbital bone invasion presents as proptosis, otherwise known as raccoon eyes (periorbital ecchymosis) (fig. 1)(41).



Figure 1. Periorbital ecchymosis in neuroblastoma

This image depicts periorbital ecchymosis - raccoon eyes- as a presenting feature of neuroblastoma in a 10 month old boy.

Source: Kapoor, 2014. (41)

1.1.4 Treatment:

A multimodal approach to treat neuroblastoma encompasses immunotherapy, differentiation therapy, chemotherapy, radiotherapy, and surgical intervention (17). This is dependent on the stage of the disease and tumour classification and whether the patient is determined as a low, intermediate, or high-risk case.

The majority of neuroblastoma patients present with unresectable or metastatic disease (17). Cases of localised tumours with positive biological profiles and localised recurrences may be treated surgically (17). Intermediate-risk cases may require a combination of chemotherapy

The Effects of Hypoxic Preconditioning on the Oxygenation and Metabolic Profile of Neuroblastoma – Yousef Al-Mutawa

and surgical resection. Cases complicated by metastasis would require chemotherapy and/or radiotherapy (17). High-risk neuroblastoma is treated intensively with a combination of chemotherapy, surgery, and radiotherapy (17). CT, MRI, and MIBG scans along with urinary catecholamine tests are used to monitor treatment response (17).

1.2 Neuroblastoma – A Biological Perspective:

1.2.1 Cancer Cell Metabolism

Metabolic activity alteration, or deregulation of cellular energetics, was designated as an emerging hallmark of cancer by Hanahan and Weinberg (2011) (fig.2A) (42). The original discovery of metabolic changes in cancer is accredited to the work of Nobel Laureate Otto Warburg in 1924 who hypothesised that cancer is caused by the tendency of cancer cells to produce ATP by non-oxidative fermentation regardless of the presence of oxygen (43, 44). To elaborate, in the presence of oxygen, normal cells produce energy via the oxidative breakdown of pyruvate in Krebs cycle generating 36 molecules of ATP per glucose molecule. In the absence of oxygen, normal cells resort to anaerobic respiration and produce energy through the less efficient breakdown of pyruvate into lactate and produces 2 ATP molecules per glucose molecule. The Warburg Hypothesis states that the tendency of tumour cells to produce energy through the latter method of glycolysis, non-oxidative glucose breakdown, regardless of the presence of oxygen is the underlying cause of cancer (Warburg, 1924). While the Warburg Effect (fig.2B) is the most prominent metabolic alteration in cancer, other metabolic changes have been identified (45). The marked increase of pyruvate kinase isoform M2, mutations of isocitrate dehydrogenase 1 and 2, and altered glutaminolysis are examples of further metabolic observations in cancer (46-48).

The Effects of Hypoxic Preconditioning on the Oxygenation and Metabolic Profile of Neuroblastoma – Yousef Al-Mutawa

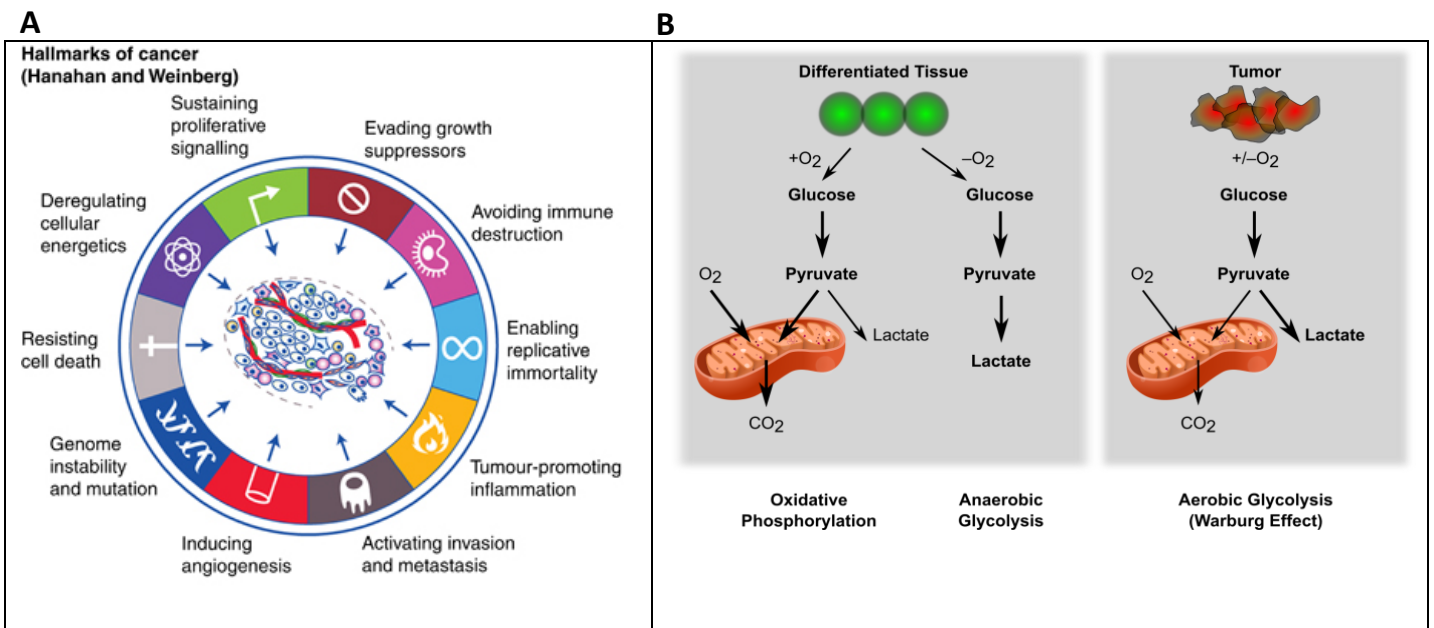


Figure 2. Metabolic Deregulation in Cancer Cells

A. Metabolic Deregulation as a Hallmark of Cancer. The Hallmarks of Cancer, as described by Hanahan and Weinberg (2011), include the deregulation of cellular energetics as an emerging hallmark. The importance of this feature was first described by Otto Warburg in what later became known as aerobic glycolysis, or the Warburg Effect (42, 49) (see fig.6).

Image credit: Hanahan & Weinberg, 2011 (42)

B. Illustration depicting cellular energy production in differentiated tissue and tumour cells. This illustration depicts the production of cellular energy via glycolysis regardless of the presence or absence of oxygen in cancer cells (right). This is known as the Warburg Effect, or aerobic glycolysis. Normal cells (left) produce energy via oxidative phosphorylation and resort to anaerobic respiration only in the absence of oxygen.

Image credit: <http://2015.igem.org/wiki/images/b/b2/ETHZ-Warburg.png> (as adapted from Heiden V. 2009 (49))

1.2.2 Metabolomics

Metabolomics is the study of the metabolites in a biological system and holds promising potential in cancer biology and biomarker discovery (50). Metabolomics provides the closest snapshot of the phenotype and function of cells and is a more recent field than the other three omics, genomics, transcriptomics, and proteomics and (51). Although the total number of human metabolites is not yet known, it is estimated to be in the tens of thousands (52, 53). The sensitivity of metabolomics and relatively low per-sample cost allow for testing a large number of samples and generating sizeable amounts of data. These factors, combined with technological advances, have kindled the interest of cancer researchers in the search for diagnostic biomarkers in serum, urine, and less commonly solid tissue samples. The value of

The Effects of Hypoxic Preconditioning on the Oxygenation and Metabolic Profile of Neuroblastoma – Yousef Al-Mutawa

metabolomics in the search for cancer biomarkers is highlighted by the multitude of literature encompassing more than 15 types of cancer (54).

Nuclear Magnetic Resonance (NMR) and Mass Spectrometry are two technical approaches in metabolomics and this study used the former approach. NMR provides higher reproducibility than mass spectrometry, albeit with less sensitivity and specificity (55). Additionally, samples require less preparation and are preserved for future analysis with NMR as opposed to mass spectrometry in which samples require more complex preparation and are destroyed (56). NMR is capable of detecting 40-200 metabolites and mass spectrometry could potentially detect more than 500 (56). High reproducibility, ease of sample preparation, short experiment duration, sample preservation, and low per-sample cost constitute the advantages of NMR spectroscopy in metabolomics. Although tumour tissue is more challenging to obtain and prepare than common bio-fluid samples such as serum and urine, research interest in direct tumour metabolomics has been increasing (52). A cancer biomarker could be measured as part of diagnostic testing, to assess tumour staging and aggressiveness, metastasis potential, and response to therapy (57).

Specifically, the metabolomics of neuroblastoma biopsy samples have been analysed to associate metabolites with patient age, prognosis, active disease, and remission (58).

1.2.3 Hypoxia

Hypoxia, or oxygen deprivation, is a characteristic feature of solid tumours defined as “a state in which the level of oxygen is decreased relative to the normal level” (59). This state of hypoxia in solid tumours is associated with an increased metastatic potential, reinforced therapeutic resistance, decreased tumour apoptosis, cancer progression, treatment resistance, and an overall poor clinical outcome (60-65).

Under hypoxic stress, the Hypoxic-Inducible Factor (HIF) transcription factor is activated triggering gene up-regulation and cellular responses to promote cell survival (66). This cellular response to hypoxia involves alteration of gene expression via the stabilisation and activation of the Hypoxia Inducible Factor (HIF) (66). In turn, this promotes cell survival by ensuring increased oxygen delivery (erythrocyte production, angiogenesis stimulation) and reduced oxygen consumption (increased glycolysis) (67-71). Erythropoietin (EPO) hormone levels

The Effects of Hypoxic Preconditioning on the Oxygenation and Metabolic Profile of Neuroblastoma – Yousef Al-Mutawa

increase to produce red blood cells and ultimately raise the oxygen carrying capacity of blood (67). Angiogenesis, the formation of new blood vessels, is stimulated by the release of vascular endothelial growth factor (VEGF) in hypoxia (68). Anti-apoptosis, tumour proliferation, metastatic potential, increased glycolysis, pH alteration, and iron imbalance are other identified cellular responses to HIF expression and hypoxia (69-76).

1.2.3.1 Causes:

Hypoxia results from a low oxygen supply and poor distribution due to weak tumour vasculature increased diffusion distances, and rapid tumour proliferation (77, 78). Dewhirst et al (2008) explains the multifactorial interplay resulting in tumour hypoxia (fig.3) (79).

The Effects of Hypoxic Preconditioning on the Oxygenation and Metabolic Profile of Neuroblastoma – Yousef Al-Mutawa

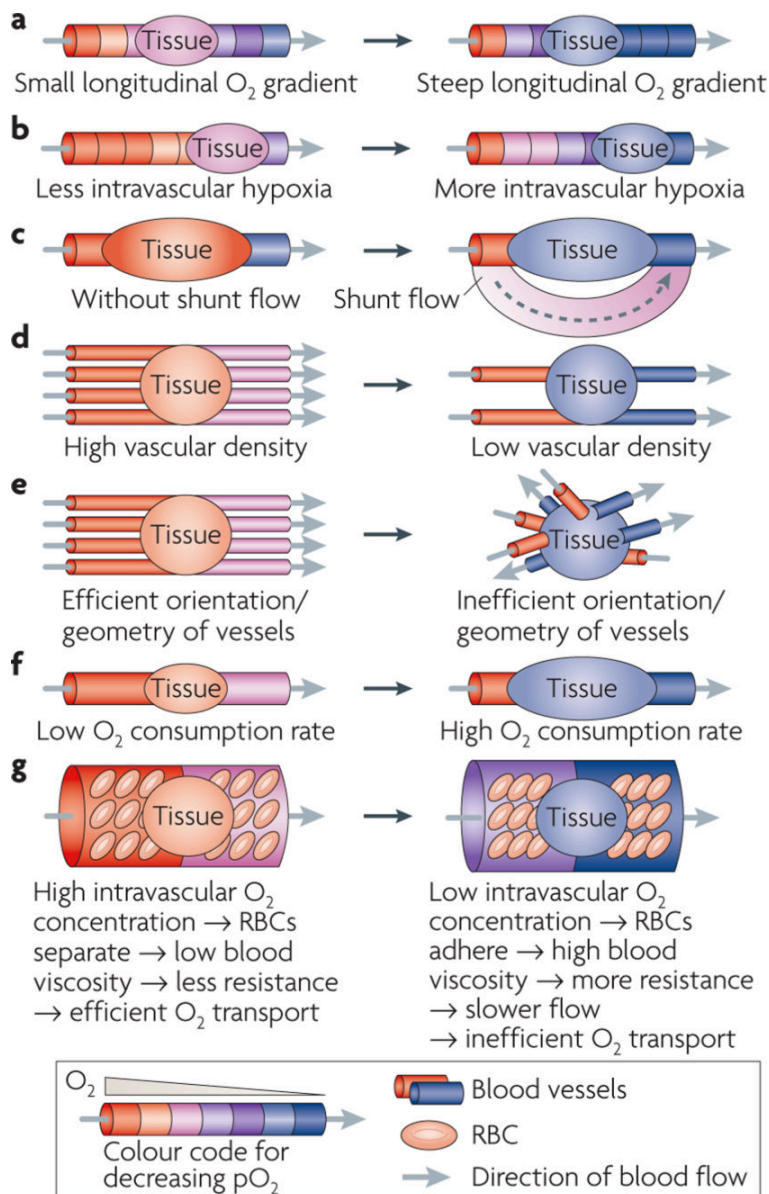


Figure 3. The 7 characteristics regulating tumour oxygenation as described by Dewhirst et al. (2008).

The intravascular drop of the partial pressure of oxygen in distal arterioles accompanied with diversion of blood flow from shunts, and restricted oxygen diffusion to the tumour along with uncoordinated blood vessel arrangements, increased oxygen demands from the growing tumour, and decreased blood flow rates due to the hypoxic effect of increasing blood viscosity all combine to result in the characteristic feature of tumour hypoxia.

Image Credit: Dewhirst et al, 2008 (79)

As a consequence of tumour growth, vasculature development, changes in diffusion distances, and unstable oxygen transportation, tumours exhibit cycling, rather than static,

The Effects of Hypoxic Preconditioning on the Oxygenation and Metabolic Profile of Neuroblastoma – Yousef Al-Mutawa

hypoxia (79, 80). The tumour microenvironment is dynamically hypoxic in that oxygen levels fluctuate in acute and chronic cycles (79). Whilst tumour hypoxia has been extensively reported as a poor prognostic marker in disease, much remains to be discovered with regards to the intracellular modifications associated with hypoxia and their link with the metastatic phenotype (81, 82).

1.2.3.2 Hypoxia and Neuroblastoma:

Hypoxia in neuroblastoma translates these biological alterations into the clinical setting and leads to chemoresistance of etoposide and vincristine, both commonly adopted chemotherapy agents (83). Moreover, recent work by Herrmann et al. (2015) utilising the chick embryo chorioallantoic membrane (CAM) model has shown that hypoxic preconditioning of *in vivo* neuroblastoma cells activates the cancer's metastasis potential and the regulation of genes supporting tumour dissemination (84). Additionally, neuroblastoma cells preconditioned in hypoxia have shown a truly fascinating phenomenon in that they trigger metastasis in adjacent cells not previously preconditioned in hypoxia and thus lack the metastatic phenotype (84). Specifically, hypoxia has been identified as an independent poor prognostic factor in neuroblastoma (85).

1.2.4 Chick Embryo CAM Model:

1.2.4.1 Introducing the model:

In vivo experimentation is a fundamental stage in research that provides more in-depth insight and translatable knowledge than *in vitro* studies as they comprise of a complete biological system in contrast to an isolated *in vitro* model that lacks vital features such as a stroma and a vascular system. Various organisms and animal models have been used for cancer research such as the murine, avian, and zebrafish models.

The chick embryo model was first exploited in the early 20th century when Rous and Murphy famously implanted Rous 45 chicken sarcoma onto the chorioallantoic membrane of the chick embryo (86). This discovery established the suitability of the CAM model for *in vivo* cancer research and tumour cell implantation to this day (87). While the mouse model would either require drug-induced immunodeficiency or special husbandry to produce genetically

The Effects of Hypoxic Preconditioning on the Oxygenation and Metabolic Profile of Neuroblastoma – Yousef Al-Mutawa

modified immunodeficient mice prior to tumour cell implantation, the chick embryo is naturally immunocompetent until embryological day 18 (87). Additionally, chick embryo experimentation up to embryonic day 14 does not require a U.K. Home Office license or ethical approval. Additionally, tumour growth on the CAM develops over a course of days as opposed to weeks in alternative animal models. Moreover, the chick embryo model is simple from a technical perspective and does not accrue high costs. This allows for a rapid, high turnover at a low expenditure.

1.2.4.2 Suitability for Neuroblastoma Research:

The distinctive feature of the chick embryo model that makes it ideal for solid tumour research is the chorioallantoic membrane (CAM). The CAM is an easily accessible, heavily vascularised extraembryonic structure that surrounds the developing embryo acting as a placenta that acts as an efficient host for tumourigenesis in that most implanted tumours complete extravasation within 24 hours, much faster than the murine model (87). Additionally, the accessibility to the tumour afforded by the CAM model allows for simple tumour cell implantation and subsequent investigations, such as tumour imaging and oxygen readings in our case.

1.2.4.3 Limitations:

A negative aspect of the chick embryo model is the loss of embryos during the process of implantation and incubation due to sensitivity to any alteration in temperature, humidity, pH, and oxygen tension (87). Moreover, chick embryos are prone to infection secondary to the opening of the shell during tumour cell implantation, which could be reduced by following standard aseptic techniques.

1.2.5 SK-N-AS Cells:

The neuroblastoma cell line utilised throughout this project is derived from a metastatic bone marrow site of a 6 year old Caucasian female diagnosed with poorly differentiated neuroblastoma in 1981 (88). Biologically, SK-N-AS cells are non-MYCN amplified neuroblastoma cells. Previous work in our laboratory by Herrmann et al. (2015) has succeeded in optimising the culture of SK-N-AS cells on the chick embryo model under hypoxic conditions (84). These cells have shown metastatic potential when pre-conditioned under

The Effects of Hypoxic Preconditioning on the Oxygenation and Metabolic Profile of Neuroblastoma – Yousef Al-Mutawa

hypoxic conditions prior to implanting upon the chick embryo. In continuity with these findings and to limit confounding variables, the same SK-N-AS cell line has been utilised in this project.

1.3 Hypothesis:

Previous work by Herrmann et al. (2015) has found that a short incubation time (72 hrs) of neuroblastoma cells in 1% O₂ resulted in a drastic phenotypic alteration of the neuroblastoma cells leading to cellular metastasis of the incubated cells suggesting a form of cellular memory of previous exposure to hypoxia (84). It is our hypothesis that hypoxic incubation causes lasting modifications in the cellular metabolome responsible for the phenotypic changes and activation of the metastatic potential in these cells.

1.4 Project Aim:

The specific targets of this study were as follows:

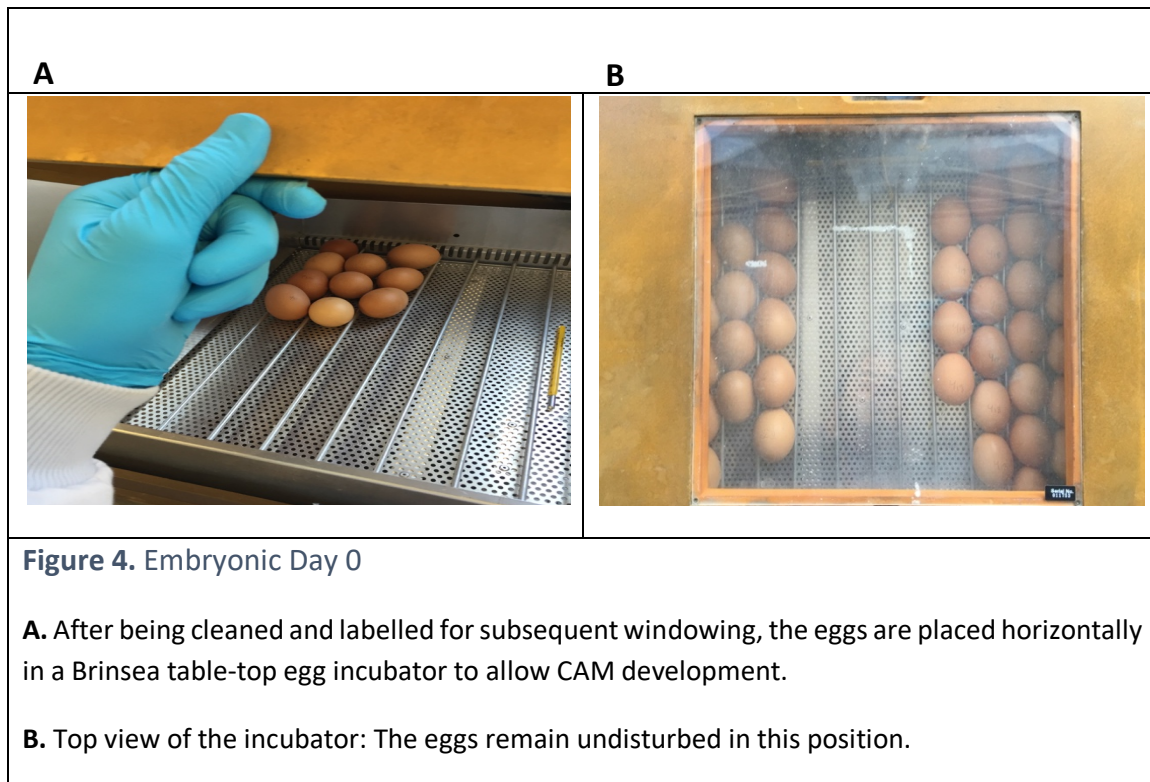
1. To record live oxygen readings of *in vivo* neuroblastoma tumours implanted on the chorioallantoic membrane of chick embryos.
2. Analyse the metabolic profile of neuroblastoma tumours, using nuclear magnetic resonance spectroscopy (NMR).
3. To compare and contrast the effects of hypoxic preconditioning of the neuroblastoma cells on the oxygenation and metabolic profiles of the neuroblastoma tumours.

2. Methods:

In this experiment, neuroblastoma cells (SK-N-AS) are implanted onto the chorioallantoic membrane and develop into a neuroblastoma tumour within 7 days (embryonic day 14). Tumours are then imaged and either undergo live oxygen measurements or harvested for metabolic profiling via nuclear magnetic resonance spectroscopy (NMR).

Cell culture reagents were purchased from Gibco (USA) and plasticware from Corning (USA) unless otherwise stated. All other chemicals and reagents were obtained from Sigma-Aldrich (USA) unless otherwise stated.

The Effects of Hypoxic Preconditioning on the Oxygenation and Metabolic Profile of Neuroblastoma – Yousef Al-Mutawa



2.1 Egg incubation:

The required number of embryonated White Leghorn chicken eggs per experiment was removed from the refrigerator (12°C) and the eggs were cleaned with a damp blue towel to remove any impurities or debris from the shell. The eggs were labelled on the long side with the date and initials to act as identifiers. They were then placed into a table-top egg incubator (Brinsea, U.K.) to lie horizontally with the labelling facing upwards (fig.4). The eggs remained in a humidified incubator for 72 h at 37°C without movement or rolling, to ensure embryo formation in the appropriate orientation. In this setup, the embryo forms beneath the labelling allowing this to be the windowing site. This incubation step marks embryonic day 0, E0 (fig.4).

2.2 Windowing:

On Embryonic day 3, the eggs were windowed in preparation for cell implantation onto the chorioallantoic membrane on Embryonic Day 7 (E7). The fume hood was prepared along with the following tools: scalpel, egg piercer, syringe, and drill. Egg trays and dividers are prepared and remain in a secondary egg incubator for the duration of windowing. The eggs were

The Effects of Hypoxic Preconditioning on the Oxygenation and Metabolic Profile of Neuroblastoma – Yousef Al-Mutawa

removed from the incubator and rolled gently by hand to detach the contents from the shell. The eggs were wiped with water and placed on the egg holder in the fume hood with the labelling facing upwards. The wide base of the eggs was pierced with an egg piercer to withdraw approximately 3 ml. of albumin withdrawn via a needle and syringe after which the piercing was covered with green tape (fig.5 A-B). The needle must be facing the inferior surface to avoid disrupting the embryo. This step is followed by drilling a rectangular window then using a scalpel to sever three sides of the shell window (fig.5 C-D). Invisible Scotch tape was attached onto the window to completely detach it from the shell and replacing it securely ensuring there are no air bubbles in the tape that would allow exchange between the inner egg and outer environment and cause disturbance to the egg's gas exchange mechanism. It was essential to form an air seal to prevent infections and improve the chance of embryo survival for the duration of the experiment (14 days) (fig.5 E). One end of the tape was kept loose to permit lifting of the window for implantation. The egg was placed into the tray in the incubator and this process was repeated until all eggs have been windowed (fig.5 F). The tray was then transferred to the primary egg incubator and disruption was avoided until embryonic day 7 for implantation. It was vital to ensure the incubator had a sufficient water supply throughout the period of incubation.

The Effects of Hypoxic Preconditioning on the Oxygenation and Metabolic Profile of Neuroblastoma – Yousef Al-Mutawa

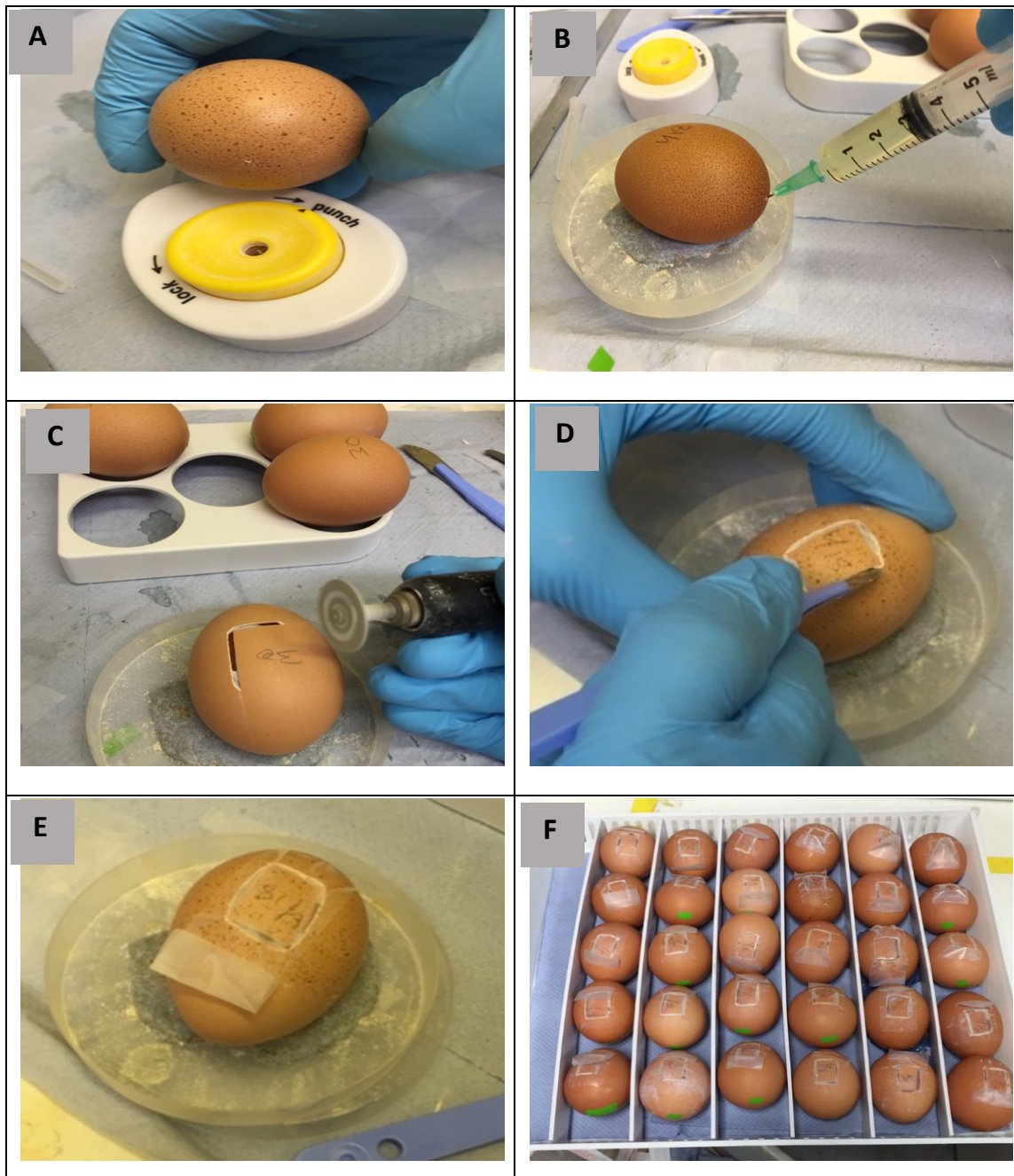


Figure 5. Embryonic Day 3 – Windowing

A. The wide base of the egg is pierced to allow insertion of a syringe needle.

B. Approximately 3ml of albumin are withdrawn from each egg causing the CAM to descend in order to allow drilling without disturbing the egg contents.

C. A rectangular window is drilled onto the eggshell above the site where the embryo has formed.

D - E: A scalpel is used to sever three ends of the window which is then sealed by Scotch tape to limit gas exchange and minimise the risk of infections and embryo death.

F: The windowed eggs are arranged in an egg tray with the windowed areas facing upwards and placed in an egg incubator.

The Effects of Hypoxic Preconditioning on the Oxygenation and Metabolic Profile of Neuroblastoma – Yousef Al-Mutawa

2.3 Chorioallantoic implantation (Embryonic day 7):

Eggs were placed under a fume hood while unfertilised and dead eggs were discarded. SK-N-AS cells were pelleted in eppendorfs and kept in ice. The number of cells to be implanted are between 2 to 4 million cells and the volume is calculated beforehand (sample calculation in table 4).

Table 4. Calculating the volume of cells to inject into the chorioallantoic membrane

| | | |
|----------------------------------|----------|---|
| Cells/ml of medium | 869000 | ← as read by the cell counter (Biorad) |
| Total ml. of media | 50 | |
| Total number of cells | 43450000 | |
| Volume of cell pellet (μ l) | 50 | |
| cells/ μ l | 8.69E+05 | By dividing total # of cells by the pellet volume |
| for 2×10^6 cells | 2000000 | (divide 2×10^6) / (cells/ μ l) |
| inject (μ l): | 2 | Volume of cells to inject in μ l |

The equipment needed for cell implantation are an optical microscope, sterile tissue paper, tweezers, and a pipette. Under the microscope, the egg window was lifted and tissue paper was inserted within the chorioallantoic membrane to create an inward fold that encloses the cells. The cells are then pipetted into the fold (fig. 6). The egg window was replaced and taped on the shell. This procedure was repeated until all eggs were implanted with the appropriate cell number and condition. Care must be taken to minimise egg movement and rotation following implantation.

The Effects of Hypoxic Preconditioning on the Oxygenation and Metabolic Profile of Neuroblastoma – Yousef Al-Mutawa

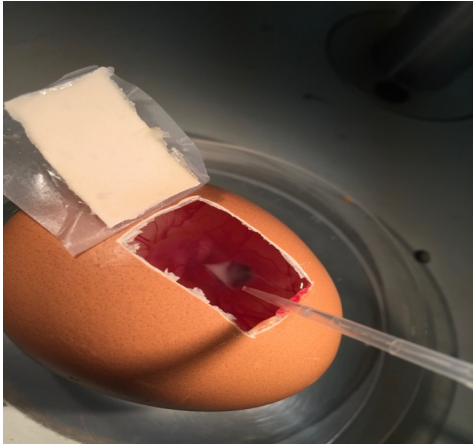


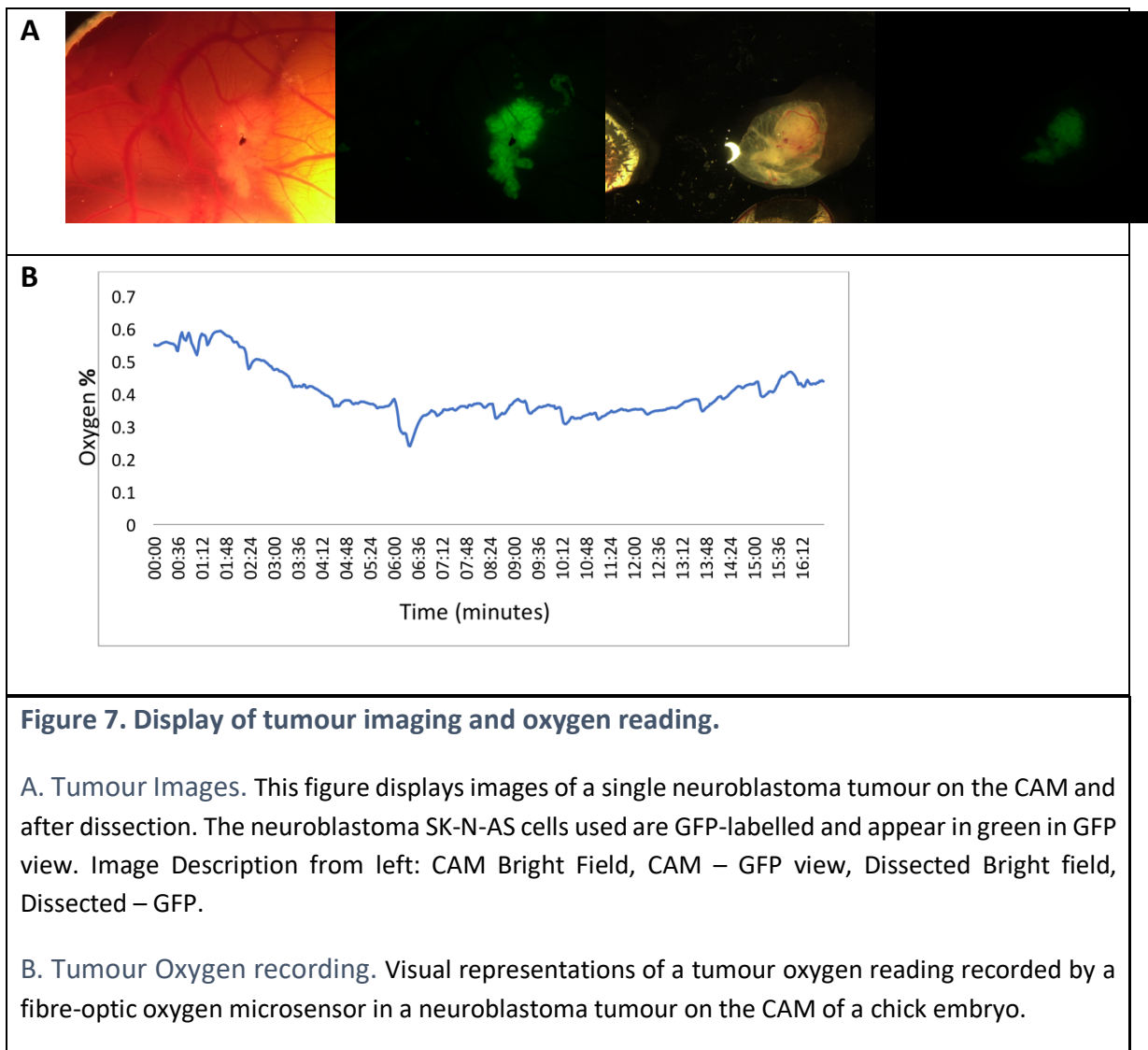
Figure 6. Embryonic Day 7 – Cell Implantation.

On embryonic day 7, SK-N-AS neuroblastoma cells are implanted onto the chorioallantoic membrane of the chick embryos. Care must be taken to ensure this step is performed in the shortest period required as the chick embryos are sensitive to disruptions in temperature and humidity.

2.4 In-vivo Oxygen Measurement:

On embryonic day 14, the oxygen tension of tumours was measured followed by tumour imaging and harvesting (fig.7). This was carried out with a Presens Microx 4 oxygen sensor device, a Needle Type Oxygen Microsensor NTH-PSt7 (Presens), a standard fluorescent stereo microscope (Leica M165FC), and a Manual Micromanipulator MM33 (Presens) (fig.8). With care to avoid breaking the egg, the shell on the side of the window was removed using tweezers to reveal the entire contents of the egg. If a tumour was present, an image of the CAM was taken in bright light and another in fluorescence (fig.7). The needle microsensor was fitted into the micromanipulator and connected to the Microx device and the temperature probe was inserted into the membrane of a control egg. Next, the needle was forwarded into the tumour and retracted slightly to allow the fibre optic sensor to be in direct contact with the tumour microenvironment (fig.8). Measurement times ranged from 15 to 40 minutes. The needle was retracted carefully from the tumour upon completion.

The Effects of Hypoxic Preconditioning on the Oxygenation and Metabolic Profile of Neuroblastoma – Yousef Al-Mutawa



The Effects of Hypoxic Preconditioning on the Oxygenation and Metabolic Profile of Neuroblastoma – Yousef Al-Mutawa

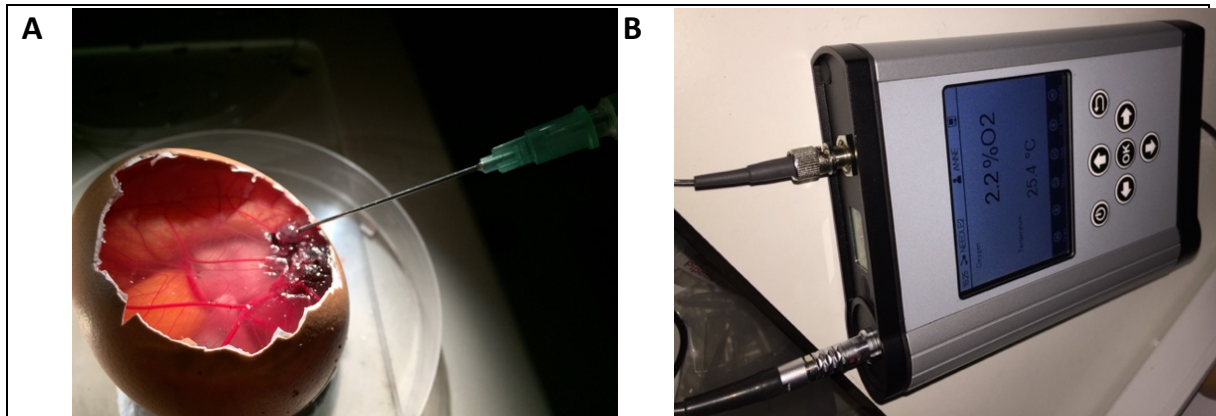


Figure 8. Embryonic Day 14 – Oxygen readings

Embryonic day 14 is the final day of the chick embryo experimentation.

A. The shell is cracked to reveal the underlying tumour and chick embryo. Under microscopic guidance, the fibre-optic needle is inserted into the tumour to detect and record live intra-tumoural oxygen readings.

B. The Presens Oxygen Microsensor displays and records the live intratumoural oxygen tension at 2 second intervals.

2.5 Tumour Extraction:

A small dissection scissor and tweezers were used to dissect the tumours from the membranes and are placed on drops of phosphate buffered saline to remove any blood after which the chick embryos were sacrificed at this point. Imaging of the tumours in bright light and fluorescence were taken in a posterior and side orientation. The method of storing tumours is dependent on the subsequent step. Both methods are explained below.

2.5.1 Tumour snap freezing (for NMR):

The tumour was weighed in an eppendorf and dropped in liquid nitrogen to freeze. The tumours are then stored in a -80°C freezer.

2.5.2 Tumours fixation and staining (for immunostaining):

Each tumour was placed in a well with 4% paraformaldehyde (PFA, Sigma) in a well plate and stored in a refrigerator for 24 hours (fig.9). The PFA was aspirated and the tumour was suspended in a sucrose gradient of 6%, 12%, and 20%, respectively. The sucrose would be

The Effects of Hypoxic Preconditioning on the Oxygenation and Metabolic Profile of Neuroblastoma – Yousef Al-Mutawa

changed every 24 hours. The tumour was then placed in a plastic embedding mould in anterior orientation (as if on the cam) and Cryomatrix (Thermo Scientific, USA) embedding solution is added. A cork top is added as a cover and the mould was placed in dry ice to freeze and subsequently stored in a -80°C freezer.

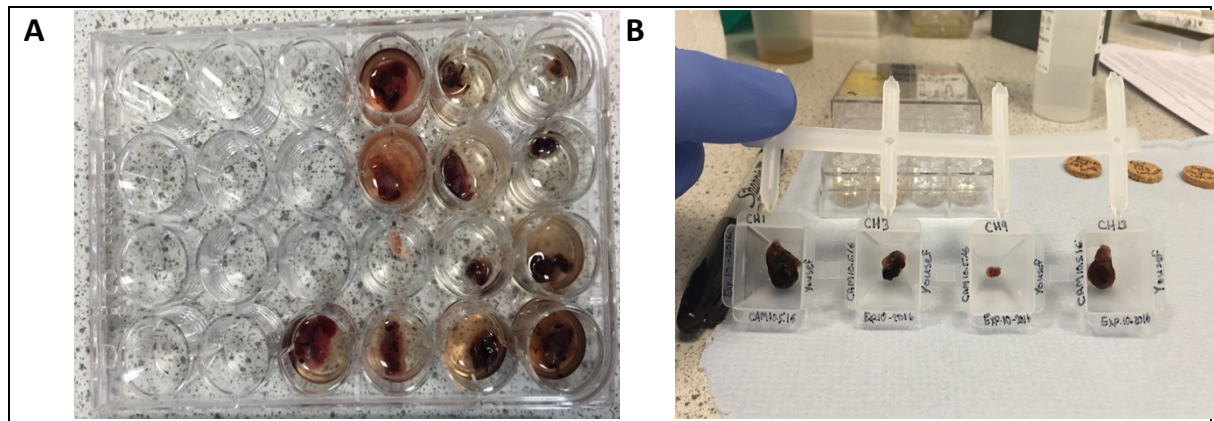


Figure 9. Tumour extraction and storage:

A. Upon extraction, each tumour is suspended in a well with 4% paraformaldehyde (PFA) and stored in a refrigerator for 24 hours. The PFA is then replaced with a sucrose gradient of 6%, 12%, and 20% respectively.

B. Tumours are then placed in a plastic mould and Cryomatrix embedding solution is added. A cork top is placed on the matrix and the moulds are placed in liquid nitrogen followed by storage in a -80°C freezer.

2.6 Tumour Slicing for Imaging:

The frozen tumours are removed from -80°C storage and kept on dry ice. A Leica CM1950 cryostat is set to slice 10µm with a temperature of -20°C. A frozen tumour mould is removed from the mould and frozen into place onto the metal specimen discs and alignment is adjusted and tested until the blade slices evenly across the specimen. The samples were collected with frosted slides (Thermo Scientific, USA) and labelled. Slices were collected from the edge and centre of the tumours. The slides were then stored in a freezer at -20°C and the sample was stored in -80°C.

The Effects of Hypoxic Preconditioning on the Oxygenation and Metabolic Profile of Neuroblastoma – Yousef Al-Mutawa

2.7 Cell culture:

EGFP and wild type human neuroblastoma SK-N-AS cells (ECACC No. 94092302) were cultured in Gibco Minimum Essential Medium (MEM) + 10%FCS + 1% NEAA. The GFP labelled cells were used for all in vivo experiments and the unlabelled (wild type) cells were used for in-vitro NMR experiments. The GFP labelling permits visualisation of the implanted SK-N-AS cells under fluorescent light.

Cells were cultured either in small T25, medium T75, or large T175 flasks depending on the output experiment. For cell culture and splitting, the volumes of reagents are indicated in table 5 below.

Table 5. Volumes of reagents required per flask size.

| Flask Size (Corning, UK) | Medium volume | 0.05% Trypsin for 1 min. | PBS volume |
|--------------------------|---------------|--------------------------|------------|
| T25 | 5 ml. | 0.5 ml. | 2 ml. |
| T75 | 20 ml. | 1 ml. | 5 ml. |
| T125 | 40 ml. | 2ml. | 5 ml. |

Cell passaging was carried out once a flask reaches confluence, typically every 2-3 days. The media was aspirated and the cells were washed with PBS, which is added with care to avoid detaching the cells. The PBS was then aspirated and 0.05% Trypsin EDTA was added for 1 minute at 37C. For CAM implantation, the detached cells were suspended in 10ml of fresh media in a falcon tube and counted with a Bio-Rad TC20 Automated Cell Counter. The tube was then centrifuged for 5 minutes at 1000rpm to form a cell pellet. The media was then aspirated and the pellet was pipetted into an Eppendorf tube and placed on ice. Cell flasks were stored in a humidified CO₂ incubator (37°C, 5% CO₂, Sanyo MC0175).

The Effects of Hypoxic Preconditioning on the Oxygenation and Metabolic Profile of Neuroblastoma – Yousef Al-Mutawa

2.7.1 Cell Collection and Freezing prior to Lipid Extraction for NMR:

SK-N-AS Cells were cultured in small T25 Corning flasks with an initial seeding at 1.00×10^6 cells in 5ml of media (MEM + 10% (v/v) FCS + 1% (v/v) NEAA) at either 21% O₂ (normoxia) or 1% O₂ (hypoxia) for 72h. The cells were harvested and counted as outlined in the cell culture methods above. They were then centrifuged in aliquots at 1000rpm for 5 minutes and the supernatant was aspirated. The pellet would be resuspended with 1 ml. PBS and the suspension transferred into an eppendorf tube which was centrifuged at 1200G for 5 minutes. The supernatant was aspirated and the remaining pellet was labelled, snap-frozen with liquid nitrogen, and stored in a -80°C freezer until extraction.

2.7.2 Calculating cell number:

Once the cells are trypsinised and neutralised with 10 ml of media, 10 µl of media is pipetted into a cell counter slide (BioRad, USA) and inserted into the cell counter (Bio-rad TC20, USA) with the parameters set between 5 and 23 micrometres. The reading is given as cells/ml. and is multiplied according to the appropriate volume.

2.7.3 Hypoxic Incubation:

Flasks were incubated in a hypoxic gas chamber (Don Whitley Scientific, 37.1°C, 1.0% O₂, 5.0% CO₂, 94.0% N₂) for 72 hours prior to implantation onto the Chorionallantoic membrane on embryonic day 7 or pellet freezing in the case of cell pellet collection for metabolomics analysis.

2.8 Immunofluorescence and Imaging:

Slides were thawed at room temperature for 10-20 minutes and a hydrophobic pen (Invitrogen, USA) was used to draw a circle around the tissue on the slides. Samples were then incubated with 50 mM NH₄Cl for 20 minutes at room temperature, followed by 30 minutes of incubation in blocking buffer at room temperature (1% (w/v) BSA, 0.1% (v/v) Triton, 0.4% (v/v) Tween20 in PBS). After the blocking step, 200µl of the primary antibody (dissolved in blocking solution) was added per sample and incubated in a humid chamber overnight at 4°C.

Upon antibody incubation, the slides underwent three 10 minute cycles of washing with blocking solution. The secondary antibody dissolved in blocking solution was then added to

The Effects of Hypoxic Preconditioning on the Oxygenation and Metabolic Profile of Neuroblastoma – Yousef Al-Mutawa

the samples (200µl per sample) for 1 hour at room temperature (Table 6). This was followed by 2 cycles of rinsing for 10 minutes with PBS. Antibody concentrations used upon optimisation are SMA 1:1000 and Antirabbit Alexafluor 555 1:2000 (table 6, supplementary fig.3).

Hoechst nuclear staining dye (1:1000) was added to the samples for 10 minutes maximum (200ul. per sample). A 5-minute wash with PBS was followed by an instant wash. The slides were dipped into distilled water, dried carefully with blue roll, and subsequently mounted with anti-fade mounting medium (DAKO, USA) and coverslips and then stored in the refrigerator for at least 1 hour before imaging.

An Epifluorescent microscope equipped with an Andor iXon Ultra 897 camera was utilised for slide imaging (Supplementary fig.3). Table 6 below outlines the antibody dilutions used and the microscope settings.

Table 6: Optimised antibody concentrations used for tumour slices staining

| | |
|----------------------|---|
| Primary antibody: | SMA 1:1000 |
| Secondary antibody: | Antirabbit Alexafluor 555 1:2000 |
| Microscope settings: | Fluorescent bulb intensity: 6 bars Exposure time (ms): GFP: 800 DAPI: 150 DSRED: 800 DIC: 10 |

2.9 Metabolomic Analysis:

2.9.1 Acetyl-Nitrile H₂O (AcN-H₂O) Tumour extraction:

Tumours for metabolomic analysis were snap frozen in eppendorf tubes immediately following tumour imaging and extraction from the chorioallantoic membrane and stored in a -80°C freezer (Sanyo Ultra Low Freezer, Japan).

The tubes were kept on ice during the acetyl-nitrile extraction. 1.2ml of ice cold AcN-H₂O was added to each sample followed by three 30 second alternating on-off cycles of sonication (MSE UK Soniprep 150 Plus Ultrasonic Disintegrator, amplitude set to 10 kHz using a microtip probe). Each sample was subsequently divided into 3 tubes to create technical replicates and centrifuged for 5 minutes at 21,500G and 4°C to remove cell debris. The supernatant was then transferred into new tubes whilst avoiding aspiration of the pellet. The centrifugation step was repeated with the same settings followed by a final transfer of the supernatant into new eppendorf tubes. The tubes were snap-frozen in liquid nitrogen and the lids are pierced before placing the samples in a lyophiliser (Thermo-Scientific, USA) for dry freezing overnight. Samples were stored in a -80°C freezer pending preparation for NMR.

2.9.2 Acetyl-Nitrile H₂O (AcN-H₂O) Cell pellet extraction:

400µl of ice cold AcN-H₂O were added to the samples. The samples were not transferred into new tubes following sonication, as for tumour samples, because the cells were already prepared in triplicates during cell culture. They were transferred after the centrifugation step. The remaining steps and settings were identical to the tumour extraction protocol outlined above.

2.9.3 Sample Preparation:

200 µl of a solution comprising of: 89.8% ²H₂O, 10% (v/v) 1mM sodium phosphate (pH 7.4), 0.1% (v/v) 100mM selectively deuterated (d₄) trimethyl silyl propionate (TSP), and 0.1% (v/v) 1.2mM sodium azide, was added per sample. Samples were vortexed for 1 minute followed by 2 minutes of centrifugation (20 °C, 12,000G). The supernatant was pipetted into 3mm NMR tubes and arranged in an NMR tube rack.

The Effects of Hypoxic Preconditioning on the Oxygenation and Metabolic Profile of Neuroblastoma – Yousef Al-Mutawa

2.9.4 NMR Acquisition:

¹H NMR spectra were acquired on a Bruker Avance III HD 700MHz spectrometer equipped with a 5mm TCI cryoprobe at pH 7.4 and 25 °C. Two 1D ¹H standard metabolomics experiments with optimal water suppression were acquired per sample; both are available in the Bruker pulse sequence library, the noesypr1d is based on the Nuclear Overhauser Effect (NOE) and the cpmgpr1d filters for small molecules via a Carr-Purcell-Meiboom-Gill (CPMG) sequence. The noesypr1d was acquired with 32 transients 20ppm spectral width, 32K points, 10ms mixing time and a 2.73 s acquisition time. The cpmgpr1d was acquired with 256 transients a 15ppm spectral width, 32K points, 9.6ms echo time and a 3.1 s acquisition time. Both spectra were acquired with a 4s interscan delay, the protein-free baseline of the cpmgpr1d resulted in these spectra used for downstream analysis.

2.9.5 Spectral Processing:

Automated data processing, Fourier transformation, and phasing were carried out in Topspin v3.2 software using standard Bruker routines. Chenomx v8.2 software used for initial metabolite identification with manual confirmation to in-house standards for metabolite peaks found to be significantly variable. The spectra were then normalised to TSP reference signal and bucketed per peak into a matrix of metabolite peak intensities using AMIX v3.9.14. Statistical analysis was carried out using R (r-project.org) both standalone and via the metabolomics server Metaboanalyst v3.0 (89).

2.10 Statistical Analysis:

2.10.1 Principal Component Analysis (PCA) and Discriminant Analysis of Principal Components (DAPC):

In order to illustrate the statistical variability between the metabolomic profiles of neuroblastoma cells and tumours, principal component analysis (PCA) is utilised. PCA is a mathematical method that reduces a large amount of variables, metabolites in this case, into smaller sets called principal components. The first principal component will identify the largest percentage of variability between the cohorts, with the subsequent principal components accounting for the remaining variability in descending order until 100% of the

The Effects of Hypoxic Preconditioning on the Oxygenation and Metabolic Profile of Neuroblastoma – Yousef Al-Mutawa

variability has been accounted for. It is a method of illustrating variance via data compression and dimensional reduction without discrimination.

Discriminant analysis of principal components (DAPC) is a statistical method introduced by Jobart et al. (2008) as a multivariate analytical tool in biological studies to illustrate differences amongst clusters, or cohorts, with minimal intra-cohort variation (90). In contrast to PCA, DAPC is a discriminant tool with prior “knowledge” of the various cohorts.

3. Results

3.1 Hypoxic Preconditioning of cells does not significantly affect oxygen tension of tumours:

In order to investigate the effect of preconditioning SK-N-AS neuroblastoma cells for 3 days in a hypoxic environment (1% O₂) on the tumour oxygenation, we performed precise live oxygen tension readings in tumours. The tumours were formed by cells cultured in either a normoxic (21% O₂) or hypoxic (1% O₂) environment. The use of a model system was essential as the collection of similar data in human tumours is complicated by technical and ethical challenges as neuroblastoma is a childhood malignancy. Subjecting ill infants to additional invasive investigations would place an unnecessary burden and stress on patients and parents in addition to resource and cost limitations.

3.1.1 Differences in Tumour Oxygenation:

In order to illustrate the test to test variability of oxygenation between the two conditions, fig.10 (A-B) displays the mean oxygen tension of each tumour as a function of their preconditioning condition and colour coded by experimental repeats. 75% (n=43) of all tumours yielded a mean oxygen tension within the range of 0-1% O₂ and 25% (n=14) were in the range of 1-3% O₂. The highest mean oxygen tension recorded was 2.74% in a tumour originating from cells preconditioned in hypoxia followed by 2.44% in a tumour from the normoxic cells.

The Effects of Hypoxic Preconditioning on the Oxygenation and Metabolic Profile of Neuroblastoma – Yousef Al-Mutawa

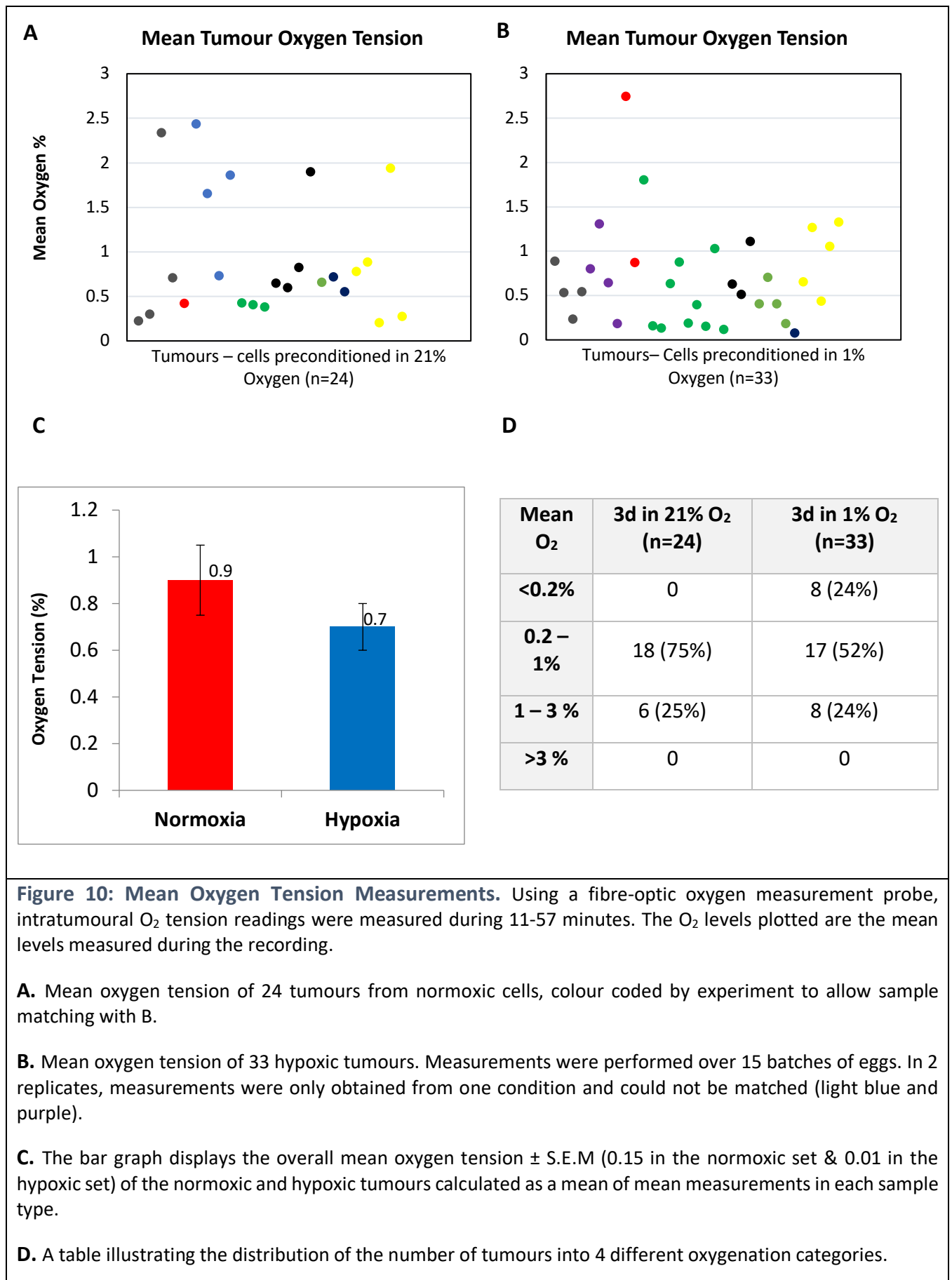


Figure 10: Mean Oxygen Tension Measurements. Using a fibre-optic oxygen measurement probe, intratumoural O₂ tension readings were measured during 11-57 minutes. The O₂ levels plotted are the mean levels measured during the recording.

A. Mean oxygen tension of 24 tumours from normoxic cells, colour coded by experiment to allow sample matching with B.

B. Mean oxygen tension of 33 hypoxic tumours. Measurements were performed over 15 batches of eggs. In 2 replicates, measurements were only obtained from one condition and could not be matched (light blue and purple).

C. The bar graph displays the overall mean oxygen tension \pm S.E.M (0.15 in the normoxic set & 0.01 in the hypoxic set) of the normoxic and hypoxic tumours calculated as a mean of mean measurements in each sample type.

D. A table illustrating the distribution of the number of tumours into 4 different oxygenation categories.

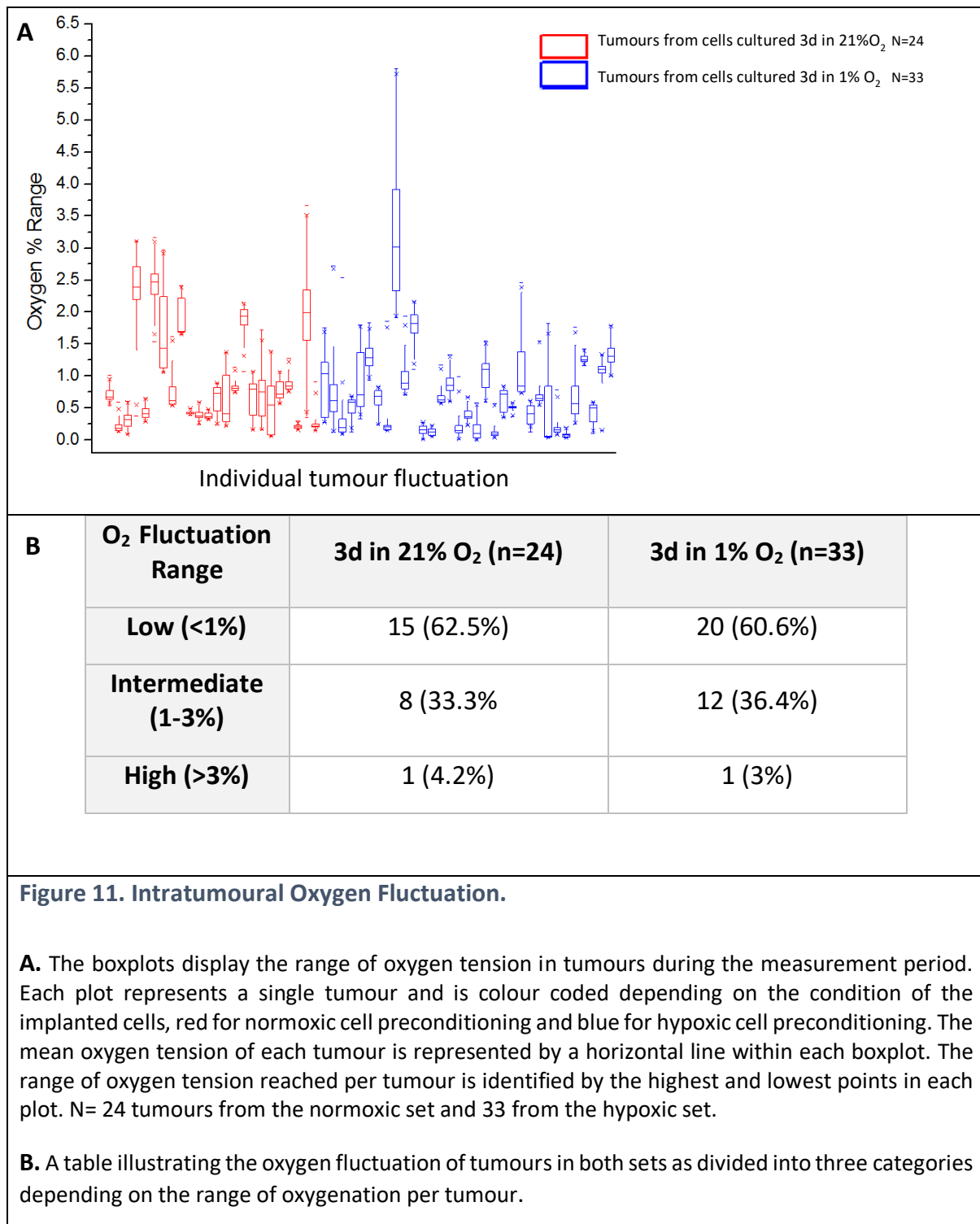
The Effects of Hypoxic Preconditioning on the Oxygenation and Metabolic Profile of Neuroblastoma – Yousef Al-Mutawa

The mean oxygen tension was slightly higher, yet statistically non-significant (p-value= 0.20), in tumours originating from cells cultured in normoxia with a mean tension of 0.9% (SD = 0.69) versus 0.7% (SD = 0.56) in tumours from cells preconditioned in hypoxia (fig.10 C). Hence, cell preconditioning in a hypoxic environment did not produce a significant subsequent effect on the oxygenation of the tumour. Moreover, both cell culture conditions generated tumours with an overall hypoxic oxygenation status.

3.1.2 Oxygen Fluctuation is not affected by hypoxic preconditioning:

To determine whether cell preconditioning affected the cycling of oxygen in tumours, the fluctuation ranges were analysed in each tumour (fig.11 A). Fluctuation ranges have been classified into three categories determined by the range of oxygen fluctuation in each tumour as follows: low (<1%), intermediate (1-3%), and high (>3%) (fig.11 B). A sample trace of a tumour oxygen reading over time is displayed in fig.7.

The Effects of Hypoxic Preconditioning on the Oxygenation and Metabolic Profile of Neuroblastoma – Yousef Al-Mutawa



Despite a slight variation, the amount of fluctuation between the two sets of tumours was consistent with 62.5% and 60.6% of tumours fluctuating less than 1% in normoxic and hypoxic tumours, respectively. Furthermore, the mean fluctuation range is 0.95% O₂ in tumours from

The Effects of Hypoxic Preconditioning on the Oxygenation and Metabolic Profile of Neuroblastoma – Yousef Al-Mutawa

cells preconditioned in normoxia and 1.03% O₂ in tumours from cells preconditioned in hypoxia.

3.1.3 Fluctuation does not increase with longer measurements:

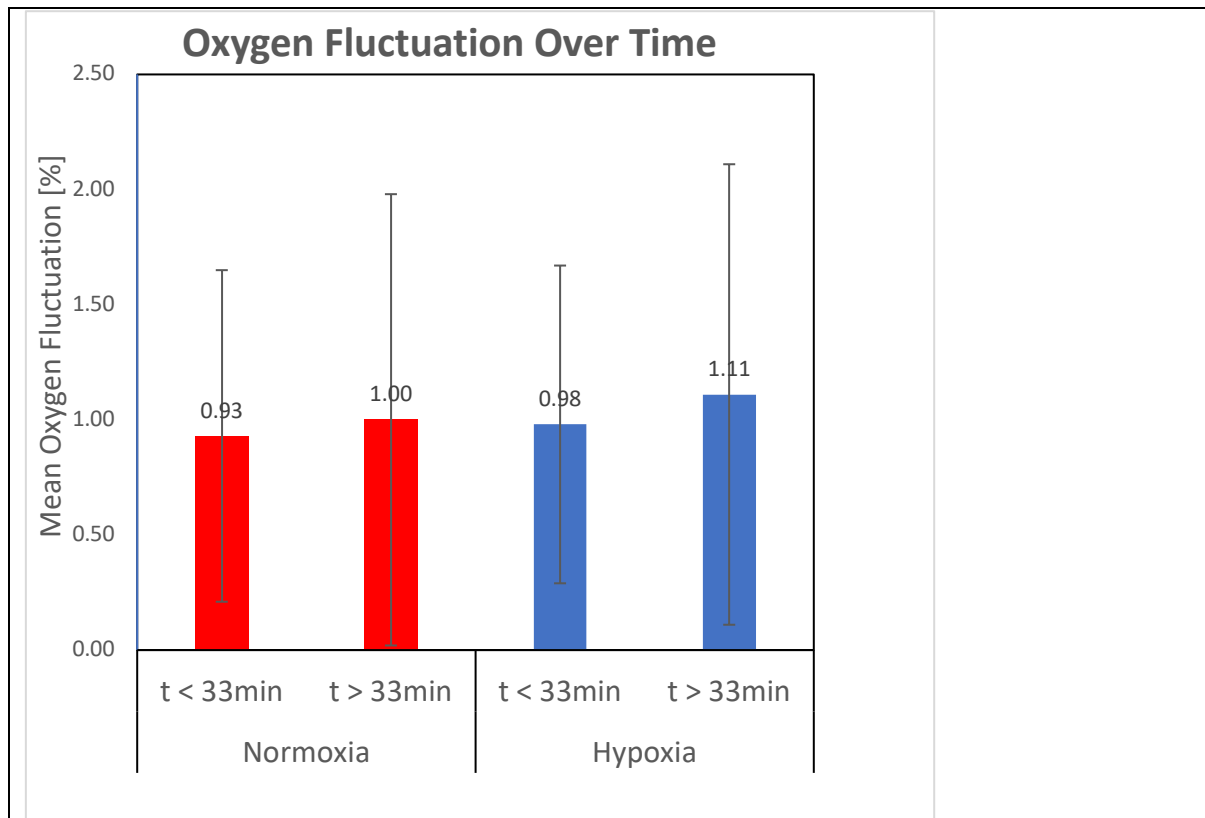


Figure 12. Oxygen Fluctuation depending on measurement time. Red and blue bars represent the mean fluctuation ranges of normoxic and hypoxic tumours, respectively. Error bars indicate the standard deviation. There is no notable difference in fluctuation over time with a 0.1% increase in range in the longer measurements within the same condition. Overall fluctuation of all the normoxic and hypoxic tumours are 0.95% and 1.0% ranges, respectively.

As hypoxic cycling can be either an acute or chronic state in tumours, we investigated whether the differences in measurement durations would under-represent cycling patterns in shorter measurements. The range of fluctuation in both tumour sets was less for measurements shorter than 33 minutes by 0.7% and 0.13% in the normoxic and hypoxic sets, respectively, compared to tumours measured for a longer period (fig.12). Hence, while the intratumoural

The Effects of Hypoxic Preconditioning on the Oxygenation and Metabolic Profile of Neuroblastoma – Yousef Al-Mutawa

oxygen status changes over time, the range of change remains similar if measured for up to an hour.

3.2 Metabolomic analysis of cell and tumour samples

3.2.1 Principal Component Analysis

To further establish the intracellular modifications triggered by hypoxic preconditioning we analysed the metabolic signature of neuroblastoma cells and neuroblastoma tumours formed on the CAM by normoxic or hypoxic preconditioned cells. NMR spectroscopy was used to identify the metabolic shift induced by hypoxia. All data are available on EBI (<http://www.ebi.ac.uk/metabolights/MTBLS541>). The spectra were divided into 354 peaks, or multiplets, of which 263 were assigned to a total of 98 metabolites. Data transformation using Principal Component Analysis (PCA) exhibited variance between the four groups of spectra with cells or tumours cultured under hypoxic conditions more varied than those under normoxic conditions (fig.13 A). As expected, the metabolic profile of cells cultured *in-vitro*, was different and well separated from cells forming tumours on the CAM *in-vivo*. Analysis of the loadings of metabolites that are most influential in the first and second principal components indicate that trehalose, glutathione and mannose together with several unidentified metabolites contribute greatest to the variance between spectra (fig.13 B). The chemical shifts of the unknown components are consistent with saccharides (whose anomeric ¹H shifts are observed between 4 and 6ppm) or molecules containing aromatic rings (shifts observed between 6 and 10 ppm).

The Effects of Hypoxic Preconditioning on the Oxygenation and Metabolic Profile of Neuroblastoma – Yousef Al-Mutawa

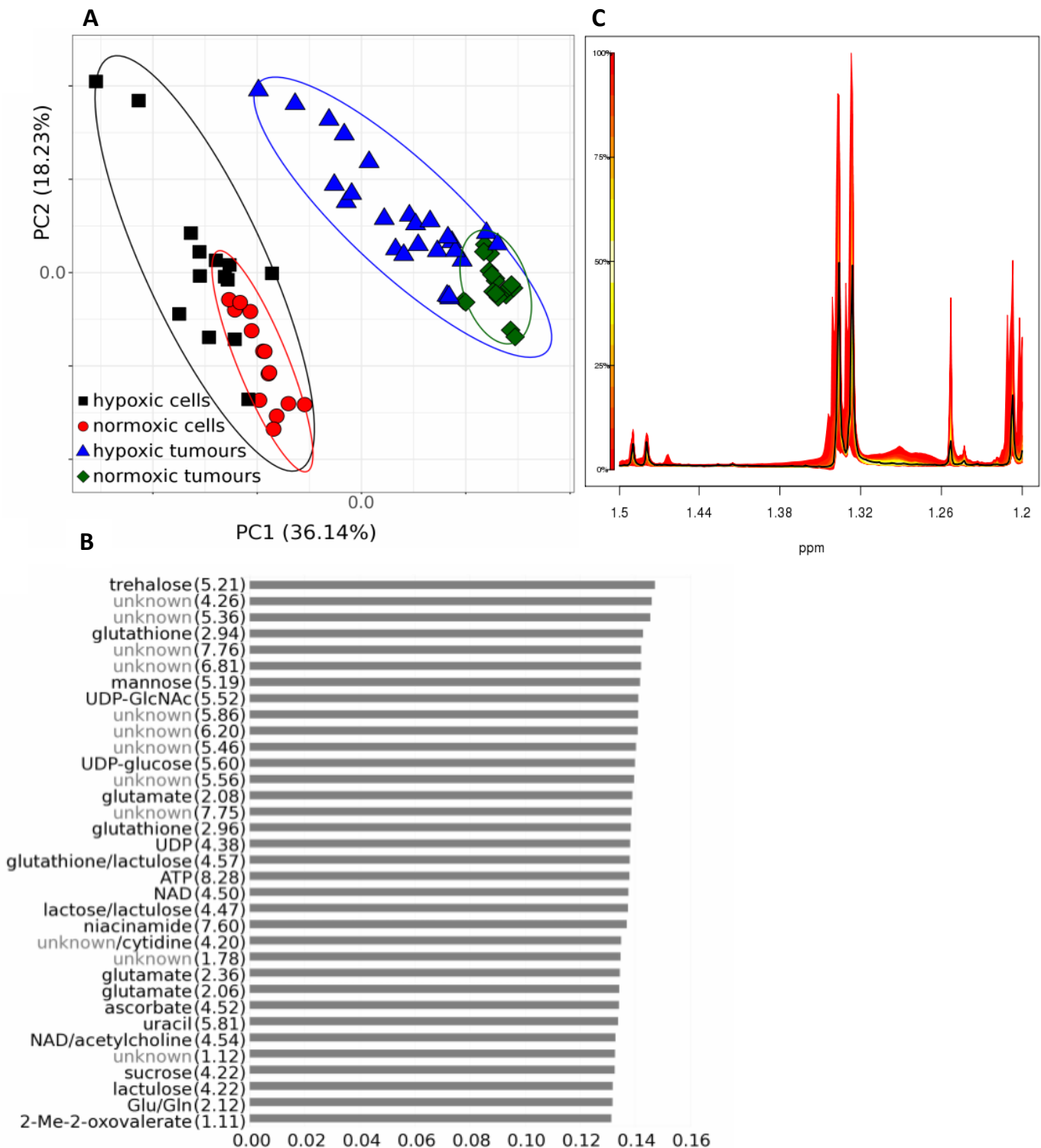


Figure 13 PCA of cell and tumour metabolite extracts.

A. scores plot shows greater variance in spectra of hypoxic samples (cells in black and tumours in blue) compared to samples cultured under normoxic conditions (cells in red and tumours in green).

B. Most influential buckets from PC1 and PC2 (combined).

C. A sample from the metabolomic analysis spectra generated by Chenomx (v8.2). A spectrum is generated for each biological sample with peaks correlating to specific metabolites. Metabolites are identified by the software library and subsequently confirmed manually. ppm = parts per million.

3.2.2 Discriminant analysis of Principal components (DAPC)

Discriminant analysis of Principal components (DAPC) was carried out to identify peaks, and therefore metabolites, responsible for spectral changes between the hypoxic and normoxic cell and tumour models (fig.14). DAPC analysis required just one linear discriminant in order to distinguish between hypoxia and normoxia in both cell and tumour models. A comparison of the top 10% signals responsible for the separation lead to the identification of metabolites that are at different abundances between normoxic and hypoxic conditions in either one or both cell and tumour systems. Taurine, choline, lactate, myoinositol, n-acetylcysteine and acetonitrile appear in both models. Creatine, glutamate, uridine, n-acetyl-ornithine, and aspartate appear in the 10% most influential buckets of the cellular DAPC model only (fig.14 B) Whereas tyrosine, 2-hydroxybutyrate, 3-hydroxybutyrate, ATP, malonate, and glutathione appear in the top 10% of the tumour DAPC model only (fig.14 D).

The Effects of Hypoxic Preconditioning on the Oxygenation and Metabolic Profile of Neuroblastoma – Yousef Al-Mutawa

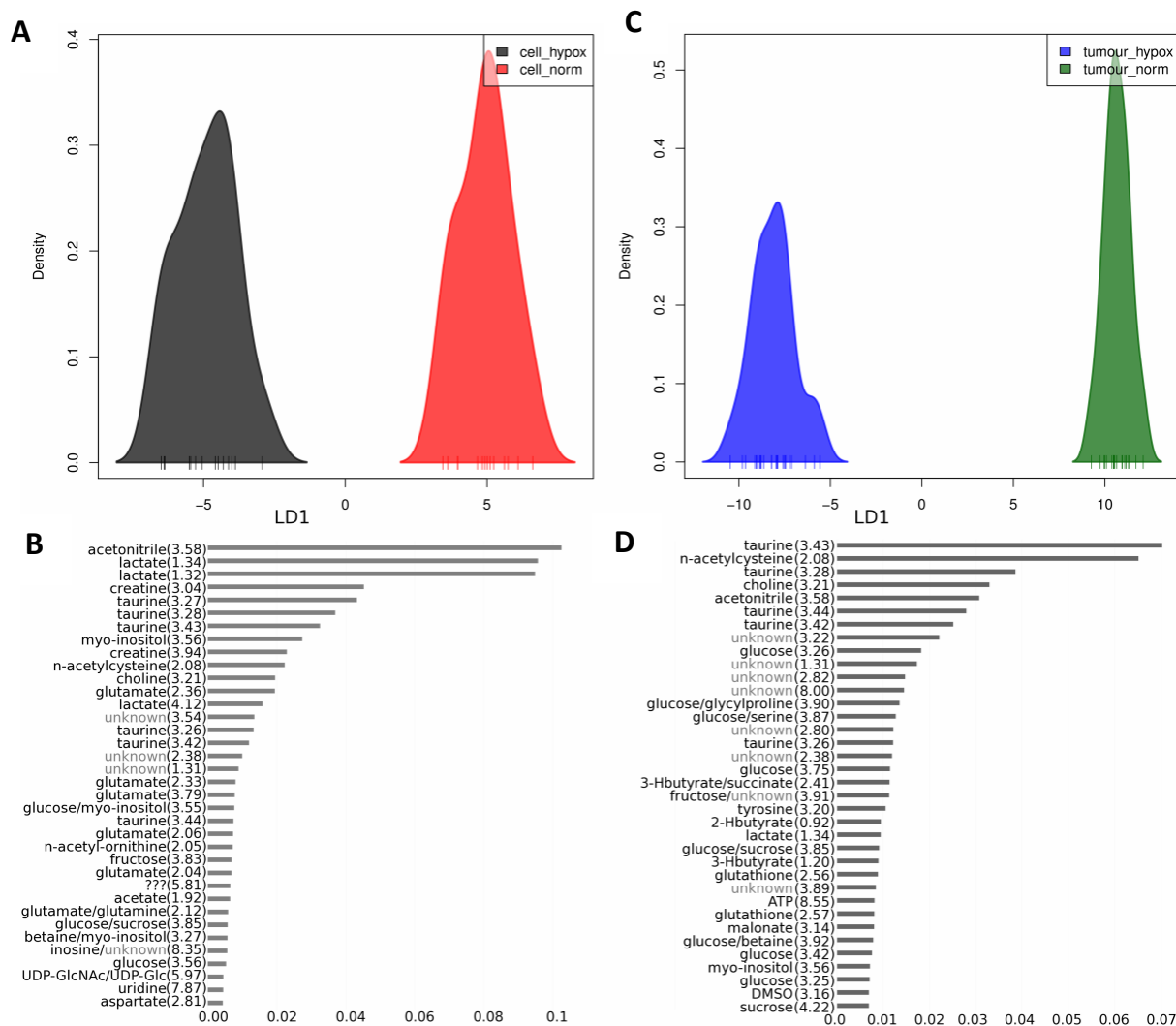
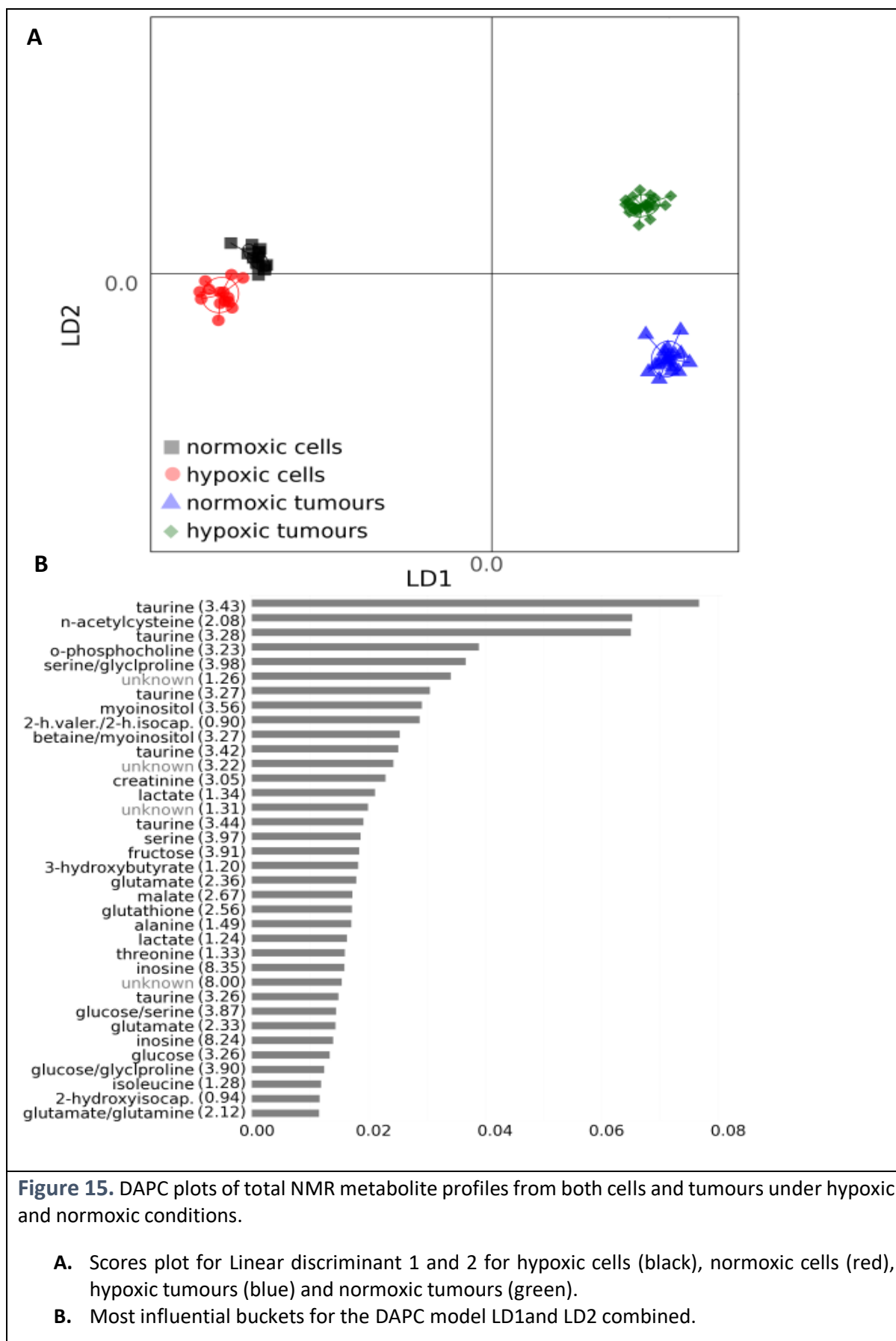


Figure 14 DAPC plots of total NMR metabolite profiles from cells (**A**, **B**) and tumours (**C**, **D**) under hypoxic and normoxic conditions. Linear discriminant 1 for **A**) hypoxic and normoxic cells shown in black and red respectively and **C**) hypoxic and normoxic tumours shown in blue and green respectively. Most influential buckets for the DAPC models for cells (**B**) and tumours (**D**).

DAPC analysis of the four conditions in one model exhibited greater differences between hypoxic and normoxic tumour profiles than between hypoxic and normoxic cell profiles (fig. 15). With the two-condition model presented in figure 14, we identified taurine, choline, lactate, myoinositol, n-acetylcysteine and acetonitrile as being influential in normoxia-hypoxia group separation.

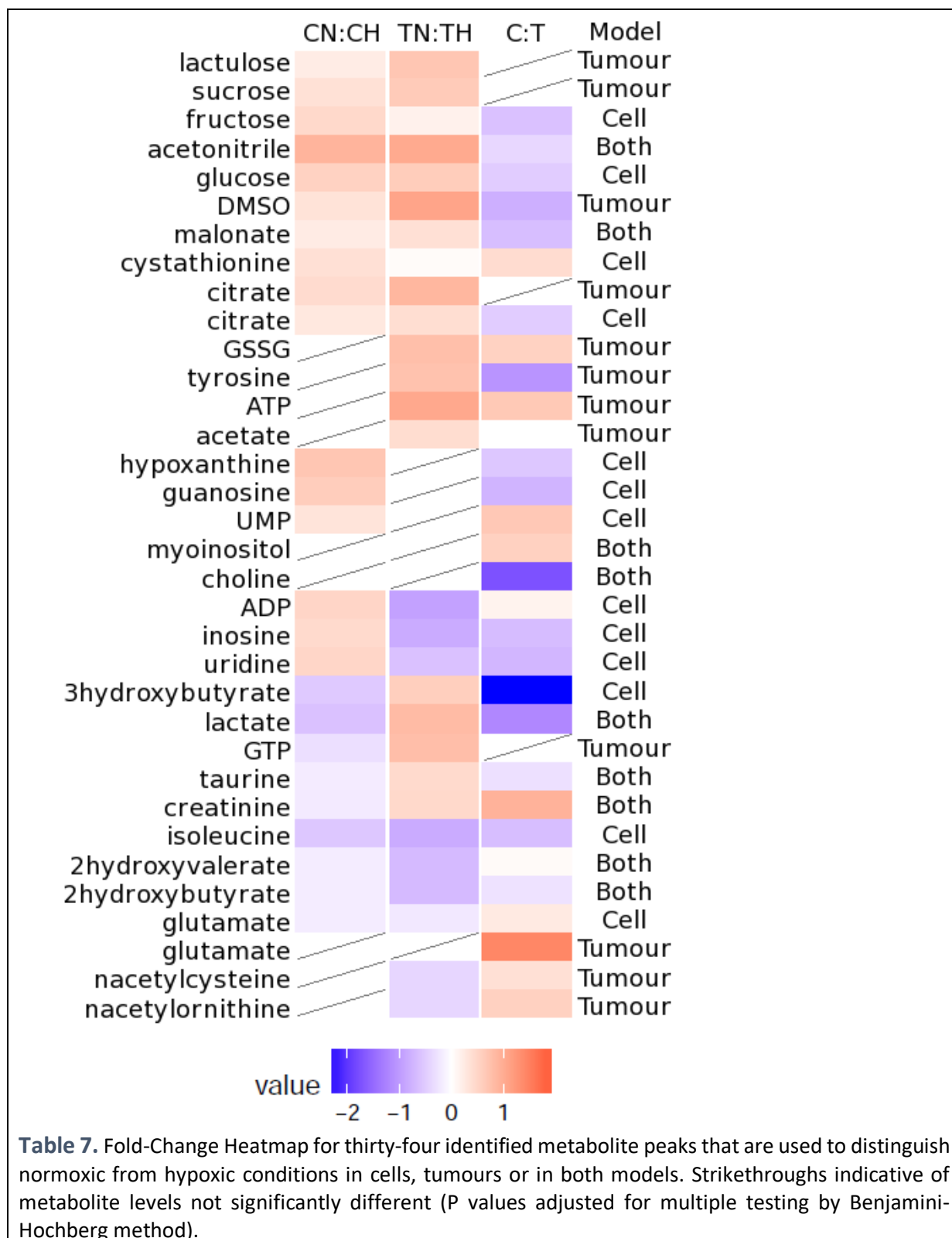
The Effects of Hypoxic Preconditioning on the Oxygenation and Metabolic Profile of Neuroblastoma – Yousef Al-Mutawa



3.2.3 Discriminant Analysis of specific metabolites to distinguish Hypoxia from Normoxia

In order to elucidate the key metabolites in the separation of hypoxic and normoxic tumours or cells, a comparison of the most influential buckets for discriminant analysis was made. From the DAPC loadings twenty-two metabolites were identified for cells and twenty-one metabolites identified for tumours with only nine of the metabolites common to both systems. This shortlist of thirty-four metabolite buckets is shown in table 7, with many exhibiting P values consistent with significantly different metabolite levels between cells or tumour conditions.

The Effects of Hypoxic Preconditioning on the Oxygenation and Metabolic Profile of Neuroblastoma – Yousef Al-Mutawa



The Effects of Hypoxic Preconditioning on the Oxygenation and Metabolic Profile of Neuroblastoma – Yousef Al-Mutawa

The shortlisted metabolites were then used exclusively to perform a Partial Least Squares Discriminant Analysis (PLS-DA) between hypoxic and normoxic conditions for either cells or tumours. The PLS-DA models for both cells and tumours were optimally fit with 5 components (cells) and 8 components (tumours) and yielded well defined separation between hypoxic and normoxic conditions with R^2 and Q^2 of 0.99 and 0.97, respectively, for the cellular model and 0.99 and 0.96, respectively, for the tumour model (fig.16). Greater variation in the metabolite profile of tumour samples (as observed in fig.13) may account for the slightly lower predictive Q^2 score.

The Effects of Hypoxic Preconditioning on the Oxygenation and Metabolic Profile of Neuroblastoma – Yousef Al-Mutawa

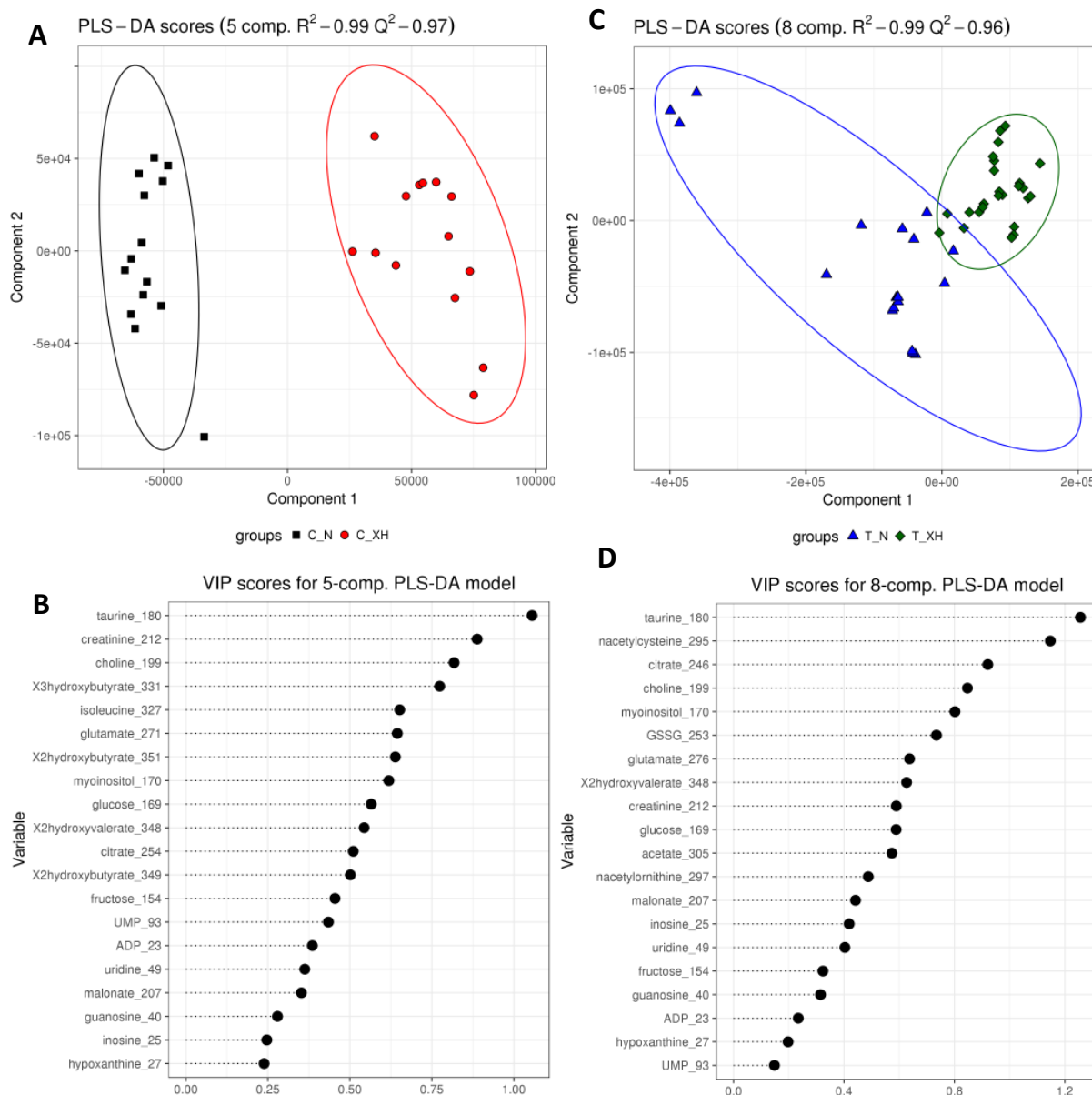


Figure 16: PLS-DA models using shortlist of metabolites for either cells (A, B) and tumours (C, D) under hypoxic (red or green) and normoxic (black or blue) conditions. Variable Influencing Permutation (VIP) scores (B and D) rank the influence of the metabolites over the model (for all components).

The Effects of Hypoxic Preconditioning on the Oxygenation and Metabolic Profile of Neuroblastoma – Yousef Al-Mutawa

3.2.3.1 Contrasting metabolite regulation between neuroblastoma cells and tumours formed on the CAM:

The most intriguing aspect of our findings are shown in the fold-change heatmap of the 34 identified metabolite peaks (Table 7). Most metabolite levels between hypoxic and normoxic conditions for the discriminating molecules exhibit differing trends between the cellular and tumour conditions (fig.17).

Of the thirty-four metabolite buckets inspected, the majority (n=10) exhibit lower levels under hypoxic conditions: lactulose, sucrose, fructose, acetonitrile, glucose, DMSO, malonate, cystathione, and citrate.

Seven metabolites are significantly higher under normoxic conditions in only cells (hypoxanthine, guanosine and UMP) or tumours (glutathione, tyrosine, ATP and acetate). Three metabolites (inosine, ADP, and uridine) are elevated in normoxic cells in comparison to hypoxic cells and are conversely elevated in hypoxic tumours when compared to normoxic tumours.

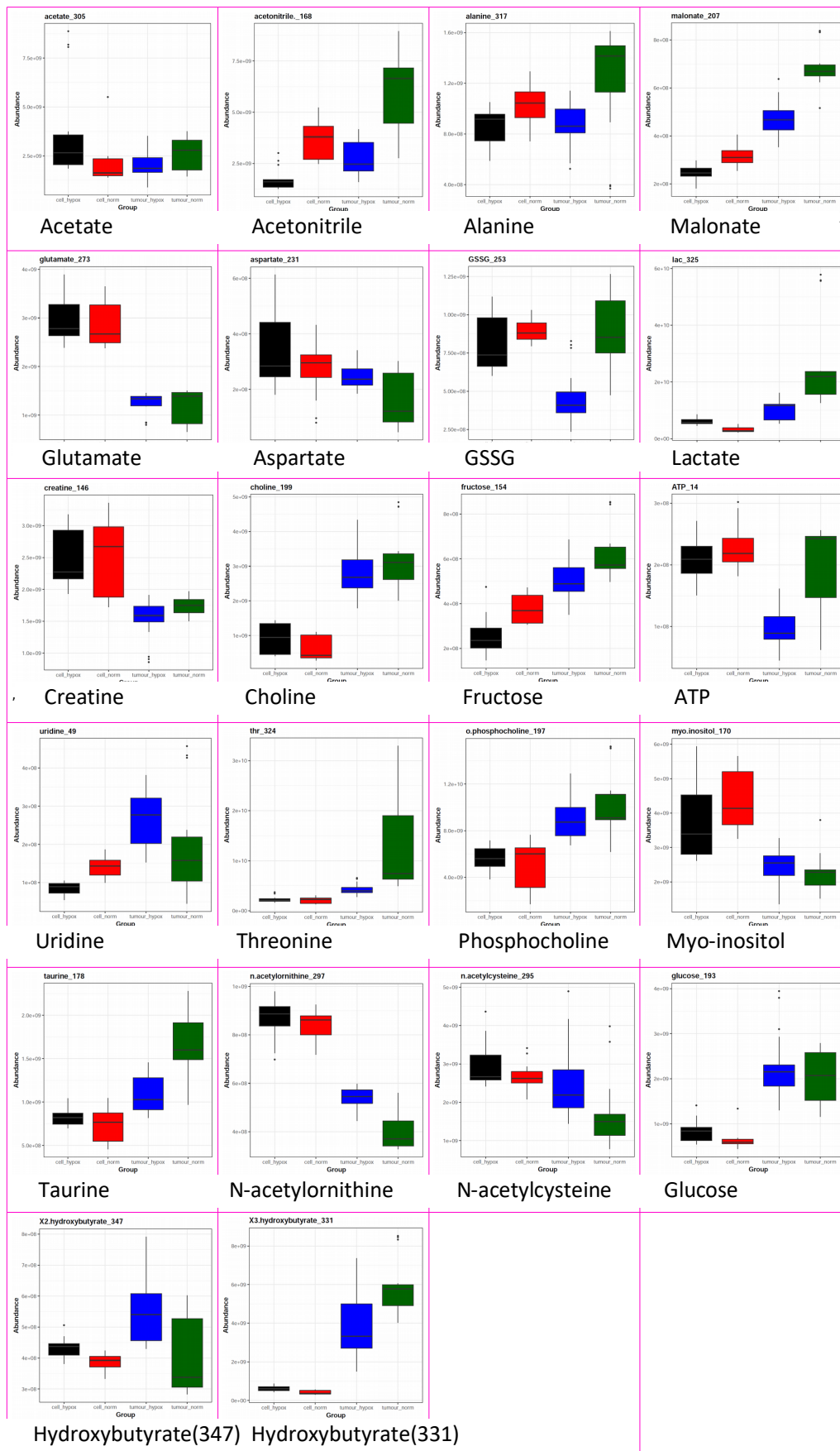
Five metabolites (3-hydroxybutyrate, lactate, GTP, taurine, and creatinine) are elevated in normoxic tumours compared to hypoxic tumours whereas, conversely, are elevated in hypoxic cells when compared to normoxic cells. In both cell and tumour extracts, four metabolites (isoleucine, 2-hydroxyvalerate, 2-hydroxybutyrate, and glutamate) are at significantly higher levels under hypoxic conditions. Myoinositol and choline are not significantly altered in either tumour or cell system however multivariate analysis has identified them as discriminant between hypoxic and normoxic conditions. This is evinced by the high VIP attributed to each in PLS-DA models, highlighting the importance of subtle distinctions not identified by crude univariate analysis.

The Effects of Hypoxic Preconditioning on the Oxygenation and Metabolic Profile of Neuroblastoma – Yousef Al-Mutawa

These metabolites can be divided into 5 categories:

- Metabolites that are more abundant in the normoxic sets of both cells and tumours in comparison to the hypoxic sets:
 - Lactulose, sucrose, fructose, acetonitrile, glucose, DMSO, malonate, cystathionine, and citrate.
- More abundant in normoxic cells vs. hypoxic cells, however, less abundant in normoxic tumours vs. hypoxic tumours:
 - ADP, inosine, uridine.
- Less abundant in normoxic cells, yet more abundant in normoxic tumours:
 - 3-hydroxybutyrate, lactate, GTP, taurine, and creatinine.
- More abundant in the hypoxic sets of both cells and tumours:
 - Isoleucine, 2-hydroxyvalerate, 2-hydroxybutyrate, and glutamate.
- Metabolites that are significantly different only within one set:
 - Only within cells: hypoxanthine, guanosine, UMP
 - Only within tumours: GSSG, tyrosine, ATP, acetate, n-acetylcysteine, and n-acetylornithine.

The Effects of Hypoxic Preconditioning on the Oxygenation and Metabolic Profile of Neuroblastoma – Yousef Al-Mutawa



The Effects of Hypoxic Preconditioning on the Oxygenation and Metabolic Profile of Neuroblastoma – Yousef Al-Mutawa

Figure 17. Boxplots of representative metabolite peaks listed in table 1 for normoxic SK-N-AS Cells (C_N), hypoxic SK-N-AS cells (C_H), tumours from normoxic cells (T_N) and tumours from hypoxic cells (T_H). Bars represent significantly difference between groups (Tukeys post-hoc analysis, adjusted P-value <0.05). Dots represent individual samples.

Colour Coding: Black = Hypoxic Cells, Red = Normoxic Cells, Blue = Tumours from hypoxic cells, Green = Tumours from normoxic cells.

4. Discussion:

This study aimed to quantify and characterise the oxygen tension and oxygenation patterns of neuroblastoma tumours developed on the chorioallantoic membrane of the chick embryo and subsequently discover the metabolomic profiles of those tumours by utilising NMR spectroscopy and specialised analytical software, R, Chenomx, and Metaboanalyst. This was an ambitious task, as to our knowledge there is no data on live *in vivo* oxygen measurements of neuroblastoma tumours. Moreover, metabolomics is a relatively new field amongst the – omic sciences (genomics, transcriptomics, and proteomics) and the advanced multivariate statistics and analytical techniques necessary to translate complex, heterogeneous chemical data into presentable results and visual representations require innovative proficiency.

The oxygen measurements and metabolomic profiling of neuroblastoma tumours are complementary investigations that allow us to identify the physiological and metabolic aspects of a neuroblastoma tumour in response to hypoxic preconditioning, instead of investigating an isolated outcome.

4.1 Tumour Oxygenation:

4.1.1 The Effect of Hypoxic Preconditioning:

The preconditioning of neuroblastoma SK-N-AS cells in a hypoxic environment for three days did not result in a significantly lower mean oxygen tension than that of the tumours that originated from SK-N-AS cells preconditioned in normoxia. Despite an absence of a significant difference (p-value = 0.2; 0.9% vs 0.69% mean pO_2 of the normoxic and hypoxic sets, respectively), the long-lasting effects of the hypoxic preconditioning are evident in the metastatic activation of tumours as shown by Herrmann et al. (2015) and by the changes in the metabolic profiles of the tumours and cells (84). The majority of tumours from both sets

The Effects of Hypoxic Preconditioning on the Oxygenation and Metabolic Profile of Neuroblastoma – Yousef Al-Mutawa

had a mean oxygen tension ranging from 0.2-1% O₂ (fig.10). It is noteworthy that no tumour from both sets has a mean oxygen tension of >3%, signifying that tumour cells exhibit a mild hypoxic microenvironment and that although hypoxic preconditioning will alter a tumour's metastatic behaviour it will not significantly impact the tumour's oxygen tension. In comparison, the median oxygen tensions of tumours as reported in the literature are as follows: Glioblastoma (0.79%), Head and neck carcinoma (1.7-2%), prostate cancer (0.34%), lung (1.05%), cervical cancer (0.42-0.71%), and pancreatic cancer (0.38%) (64).

4.1.2 Oxygen Fluctuation:

By the late 1980s, several measurement techniques such as NMR spectroscopy and polarographic electrodes were being utilised for tumour oxygen measurements with variable rates of sensitivity and success (91). Of relevance, Chaplin et al. (1986) observed that tumour hypoxia can transpire as chronic, diffusion-limited hypoxia or acute, transient hypoxia (92). This phenomenon of dynamic and heterogeneous tumour hypoxia has been further evaluated and confirmed by ensuing research (79, 93).

Hence, it was necessary to investigate whether longer tumour oxygen measurements would highlight notable differences in the cycling of hypoxia and whether we would detect higher ranges of fluctuation within a tumour with longer readings. Our *in vivo* oxygen tension recordings of neuroblastoma tumours confirm the dynamic state of tumour oxygenation in both tumour sets (fig.11 A). However, hypoxic preconditioning of tumour cells did not seem to exaggerate or decrease the range of fluctuation (fig.11 B). Our fluctuation results reflect the findings of Brurberg et al. (2005) which did not show any correlation between oxygen fluctuation and oxygenation status of canine tumours (94).

Together, these data confirm that oxygen levels in neuroblastoma are fluctuating and that the metastatic phenotype, acquired by hypoxic preconditioning, results in a slightly lower overall mean of oxygen levels without influencing the occurrence of cycling hypoxia. The spatial and temporal heterogeneity of our neuroblastoma tumour oxygen measurements are consistent with the characteristics of tumour oxygen measurements in the literature (64, 77, 79, 95, 96).

The Effects of Hypoxic Preconditioning on the Oxygenation and Metabolic Profile of Neuroblastoma – Yousef Al-Mutawa

4.1.3 Limitations of oxygen measurements:

The limitations with respect to gathering tumour measurement recordings were represented by the variability in tumour sizes which posed technical challenges in placing the fibre-optic sensor via the micromanipulator precisely within the tumour without causing tumour haemorrhage or tissue damage. Chick movements during the recording period may result in artefact fluctuations by slightly changing the needle's position. Additionally, time was a limiting factor and it was not practical to gather longer oxygen readings with the number of tumours to be recorded in each experimental setup.

4.2 Metabolomics:

4.2.1 Principal component analysis (PCA)

Principal component analysis (PCA) was utilised to illustrate the variance between the four experimental conditions (cells and tumours divided into either normoxic or hypoxic preconditioning). Interestingly, greater variance was shown between oxygenation conditions rather than the biological systems. Both the cells and tumours from the normoxic set clustered more closely than the cells and tumours of the hypoxic set. This may signify the underlying metabolic disruptive effects of hypoxia on both an *in vitro* and *in vivo* level.

Trehalose, the most influential metabolite from Principal components (PC) 1 and 2 combined, is a disaccharide known for its resistance to acidic conditions (fig.13 B) (97). Glutathione, a metabolite formed from cysteine, functions as a cellular antioxidant defense mechanism and as an enzymatic coenzyme and has been directly linked to carcinogenesis and chemoresistance (98, 99). Increased glutathione levels have been found to contribute to the resistance to oxidative stress characteristic of tumour cells (99). The third most influential identified metabolite in PC1 and 2 is mannose, a carbohydrate molecule (fig.13 B). Furthermore, boxplot representation (fig.18) reveals mannose to be more abundant in hypoxic cells and tumours than their normoxic counterparts. This correlates with the findings of Kotze (2012) which showed decreased mannose in normoxic tumour cells in comparison to hypoxic preconditioned cells (100). Recently, mannose receptors have been identified as transport proteins on tumour-associated macrophages (TAM) and are being utilised in cytotoxic drug delivery and *in vivo* tumour imaging (101-103).

The Effects of Hypoxic Preconditioning on the Oxygenation and Metabolic Profile of Neuroblastoma – Yousef Al-Mutawa

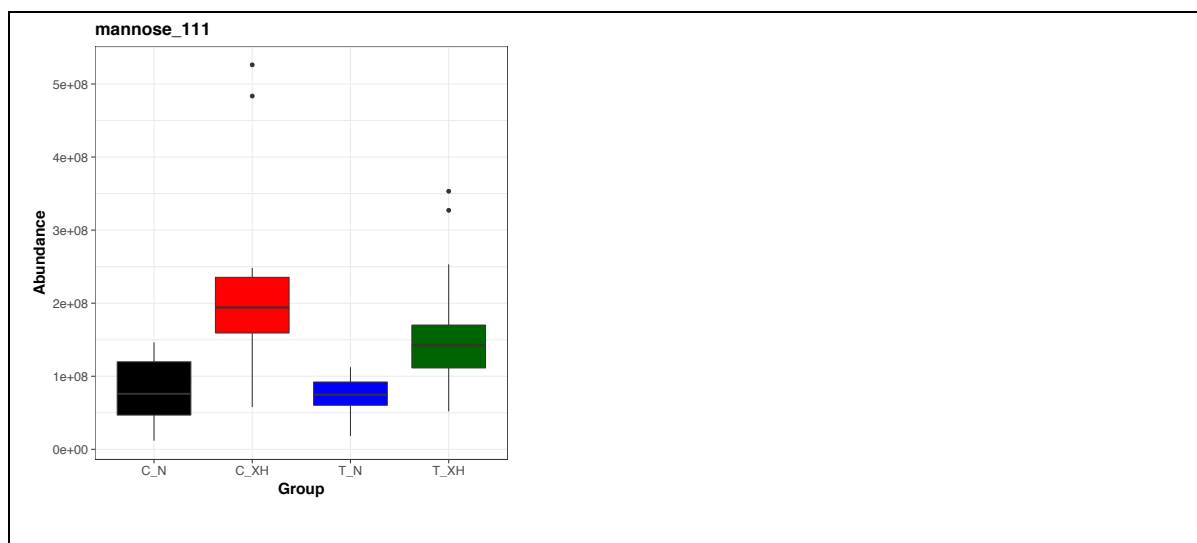


Figure 18. A boxplot representation illustrating the contrasting abundance of mannose in both cells and tumours. Colour Coding: Black = Hypoxic Cells, Red = Normoxic Cells, Blue = Tumours from hypoxic cells, Green = Tumours from normoxic cells.

While PCA showed greater variance between hypoxic and normoxic conditions rather than between cells and tumours, discriminant analysis revealed a greater variance between hypoxic and normoxic tumour sets than between cells.

4.2.2 Heatmap:

Our results showed increased levels of lactate in the hypoxic cells in comparison to the normoxic cells which is an expected finding in line with the Warburg Hypothesis of aerobic glycolysis (42, 49). However, in tumours, we detected higher levels of lactate within the tumours originating from normoxic cells. Although, it is noteworthy to recall that unlike the cells, all of the tumours exhibited a hypoxic microenvironment regardless of hypoxic preconditioning of the cells as illustrated by our oxygen measurements (fig.10).

Although more detectable in cells than in tumours, there was no significant difference in myo-inositol levels amongst both sets. However, myo-inositol was found to be decreased in response to tumour hypoxia in breast cancer and increased in neuroblastoma biopsies (58, 104).

The Effects of Hypoxic Preconditioning on the Oxygenation and Metabolic Profile of Neuroblastoma – Yousef Al-Mutawa

In contrast to the findings of Tsai et al. (2013), glutamate levels were increased in the hypoxic sets of both cells and tumours (104). Higher glutamate levels in response to hypoxia were also detected in human glioblastoma cells and in Stage I-II neuroblastoma biopsies (58, 105).

Taurine and choline are amongst the metabolites responsible for spectral separation in both cells and tumours (fig.14). Interestingly, NMR spectroscopy of neuroblastoma samples detected increased levels of taurine in patients with a poor prognosis (58). Additionally, increased concentrations of taurine and choline have been detected in colon cancer and in response to hypoxia in human glioblastoma cells (105, 106). Our results showed higher levels of taurine in hypoxic SK-N-AS cells than in normoxic cells. Conversely, the pattern is reversed in tumours, with higher taurine levels in tumours originating from cells cultured in normoxia. Moreover, there was no significant difference in the levels of choline between the normoxic and hypoxic cells and tumours. However, choline was more abundant in tumours than in cells.

It is likely that DMSO and acetonitrile are products of the culture media and extraction lysate, respectively. Multiple carbohydrates, citrate, and ATP are also lower under hypoxic conditions, consistent with productive glycolysis and the citric acid cycle in normoxic conditions when compared to oxygen deprived environments. Lower nucleotide levels (inosine, ADP, and uridine) in hypoxic cells may suggest reduced protein production and biosynthesis in comparison to cells cultured in a normoxic condition. Isoleucine, 2-hydroxyvalerate, and 2-hydroxybutyrate were found to be significantly higher in the hypoxic sets of both cells and tumours. These metabolites have been associated with lactic acidosis and associated metabolic diseases (107-109). Interestingly, hydroxybutyrate, a ketone body, has been associated with the acceleration of tumour growth and tumour inhibition in what has been termed as the 'butyrate paradox' (110, 111). Unsurprisingly, the majority of metabolites are detected at higher levels in tumours than in cells irrespective of oxygen levels with notable exceptions being media components glutamate, creatinine, and ATP.

Moreover, various notable metabolites not identified in our findings have shown a significant reaction to tumour hypoxia in the literature of which some are: glutamine, phenylalanine, valine, leucine, methionine, pyruvate, formate, creatine, alanine, creatine phosphate, and proline (58, 104, 105). Additionally, a recent meta-analysis of clinical metabolomic studies encompassing 18 types of cancer confirmed the finding of increased glycolysis and highlighted

The Effects of Hypoxic Preconditioning on the Oxygenation and Metabolic Profile of Neuroblastoma – Yousef Al-Mutawa

metabolites previously less associated with cancer such as histidine and tryptophan, both of which have not been detected in our data (112).

Whilst the cellular experiments reflected the expected metabolic changes in accordance to the Warburg Effect with higher levels of lactate in the hypoxic sets, it becomes more complex to ascertain in our tumour analysis (49, 112). Firstly, the cell is an isolated system whereas the tumour samples are heterogeneous in size and contents of tissue, stroma, and vasculature. Additionally, the hypoxic effects are more pronounced in the cellular experiments as the comparison was made between normoxic and hypoxic cells. Moreover, our experiments have shown that while the effects of hypoxic preconditioning of the cells persisted in the phenotype and metabolic profiles of the tumours, the oxygenation of the tumours was not effected and both tumour sets had hypoxic microenvironments.

Although, from a clinical perspective, tumour samples derived from different hosts are heterogeneous with varying microenvironments, it was necessary to eliminate any confounding variables in preparing and analysing the *in-vivo* samples by following standardised extraction procedures. Developing rigorous protocols is a necessity in NMR research as metabolomic analysis is easily affected by sample preparation and host variation (56). The advantages of our approach to tumour metabolomics analysis lie in the number of tumours extracted, stored, and analysed in a standardised environment and protocol. The standardised, controlled, and high throughput advantage gained from the chick embryo model provides efficient replication with limited sample degradation and avoids the drawback of running metabolomic analysis on aged clinical tumour samples stored for years (113). Additionally, our protocol divides each tumour into a triplicate during extraction to test reproducibility, identify sample differences, and validate our findings.

Understandably, the majority of studies focus on metabolite profiling of biofluids such as serum and urine as these samples are easily obtainable and do not involve invasive or surgical procedures as would be the case in tumour biopsies. This study provides insight on the metabolic profile directly from the epicenter of the disease rather than the biofluids produced secondary to it.

5. Conclusion:

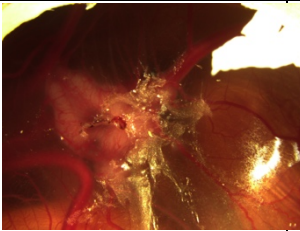
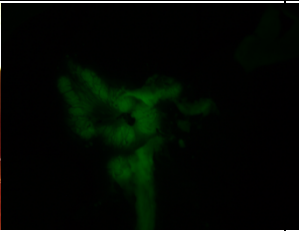
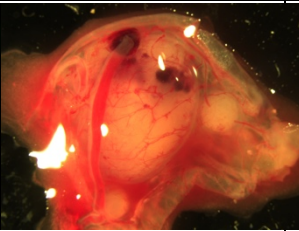
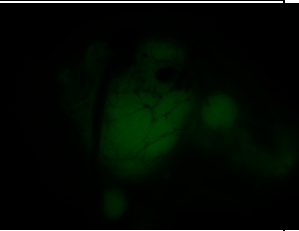

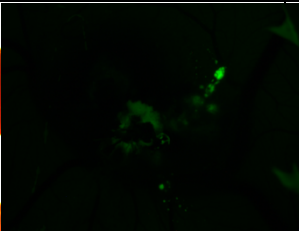
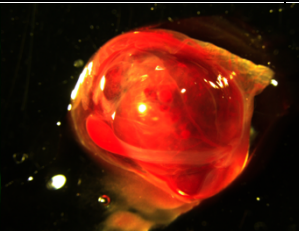
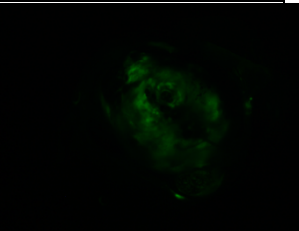

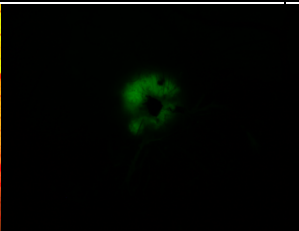
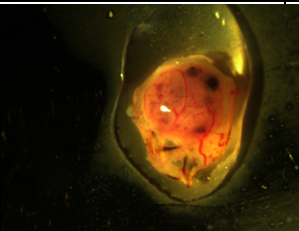
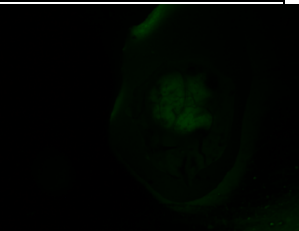
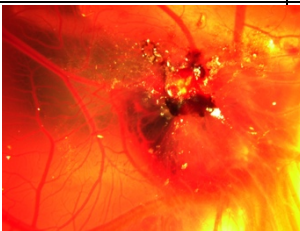
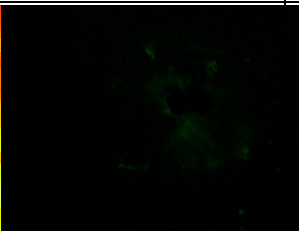
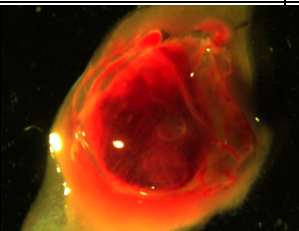
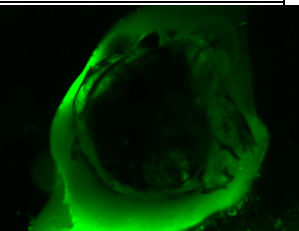
Manipulation of oxygen levels in a preclinical model has shown that in addition to altering the phenotype of SKNAS cells by inciting aggressive metastasis, certain metabolic shifts are evident in in-vitro and in-vivo models as a result of hypoxic preconditioning. The crucial knowledge gained from the oxygen readings is that the distinction between normoxia and hypoxia is not reflected in tumour oxygenation and that the measured neuroblastoma tumours are essentially hypoxic environments regardless of cell preconditioning. Hence, the comparison of metabolite intensities in tumours is effectively between the tumour history and the status of the cells used to form them.

The implications of these findings are the enduring biological effects triggered by hypoxia on cancer cells even prior to tumourigenesis. To our knowledge, this is the first study to investigate the differences in the metabolomic response to hypoxic preconditioning in cells *in vitro* and *in vivo* tumours.

The new aspects provided in this study supplement previous work by Hermann et al. (2015) on the direct link between cellular hypoxia and tumour metastasis and extend the concept of cellular memory of hypoxia into metabolite activity (84).

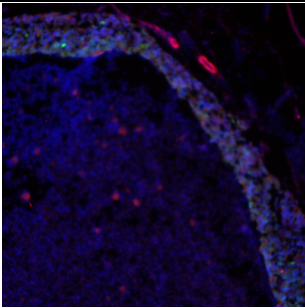
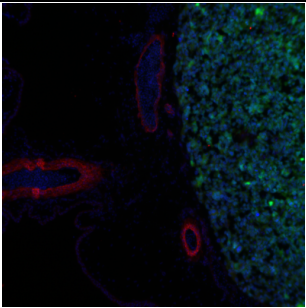
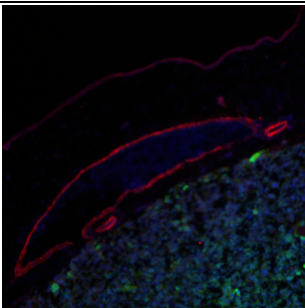
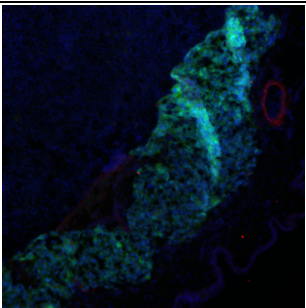
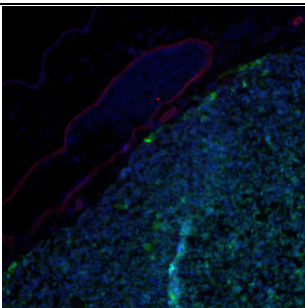
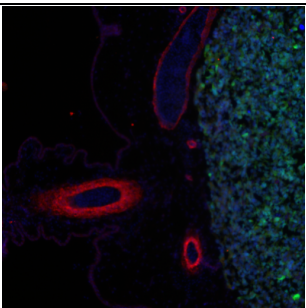
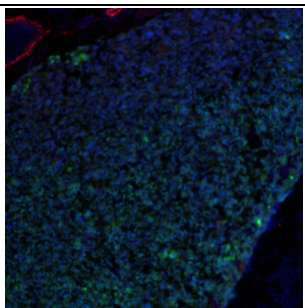
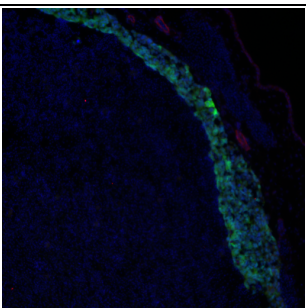
The idea of metabolic alteration as a hallmark in cancer biology dates back to Otto Warburg's discovery in the early 20th century of altered lactate production in cancer. Continuous research efforts are now focussed on metabolomics as the biological discipline that may allow the discovery of tumour biomarkers that will aid in early detection and disease stratification in cancer. However, the early findings tend to be broad and descriptive before the investigatory tools are advanced enough to provide precise answers and solutions.

6. Appendix:

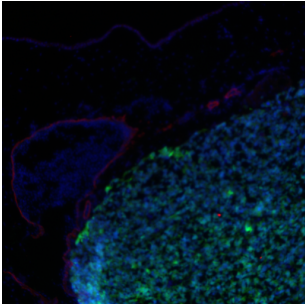
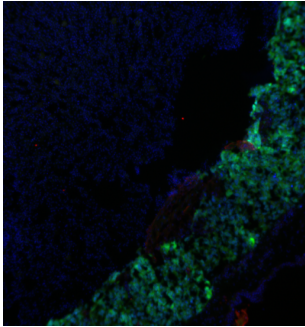
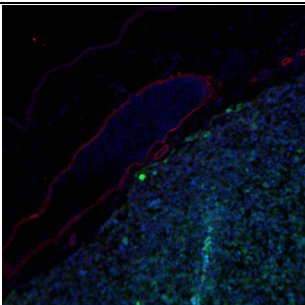
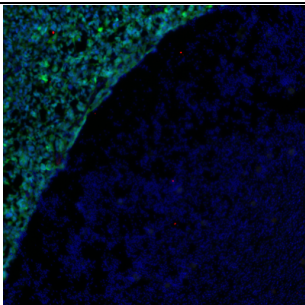
| Supplementary Figure 2 – Tumour Images in Bright Field & GFP | | | |
|---|---|--|---|
| CAM Bright Field | CAM GFP View | Dissected Bright Field | Dissected GFP View |
|  |  |  |  |
|  |  |  |  |
|  |  |  |  |
|  |  |  |  |

Supplementary Figure 3. This figure displays images of the neuroblastoma tumours on the CAM and after dissection. They are shown in bright field and GFP views. The neuroblastoma SK-N-AS cells used are GFP-labelled and appear in green in GFP view.

Supplementary Figure 3: Immunofluorescent Imaging of Tumour Sections

| | | |
|----------|---|--|
| A |  |  |
| B |  |  |
| C |  |  |
| D |  |  |

The Effects of Hypoxic Preconditioning on the Oxygenation and Metabolic Profile of Neuroblastoma – Yousef Al-Mutawa

| | | |
|--|---|--|
| E |  |  |
| F |  |  |
| <p>Supplementary Figure 4. This figure shows tumour cell intravasation. Tumour sections have been stained with various concentrations of primary (SMA) and secondary (Antirabbit 555) fluorescent antibodies. The GFP-labelled SK-N-AS cells appear in green, cellular nuclei appear in blue, and vessels appear in red.</p> <p>Antibody concentrations are as detailed below:</p> <ul style="list-style-type: none">A. SMA 1:1000 555 1:2000B. SMA 1:1000 555 1:1000C. SMA 1:800 555 1:600D. SMA 1:800 555 1:1000E. SMA 1:800 555 1:2000F. SMA 1:400 555 1:600 | | |

The Effects of Hypoxic Preconditioning on the Oxygenation and Metabolic Profile of Neuroblastoma – Yousef Al-Mutawa

7. References:

1. Maris JM, Hogarty MD, Bagatell R, Cohn SL. Neuroblastoma. *Lancet*. 2007;369(9579):2106-20.
2. Sharp SE, Gelfand MJ, Shulkin BL. Pediatrics: Diagnosis of Neuroblastoma. *Seminars in Nuclear Medicine*. 2011;41(5):345-53.
3. Angstman KB, Miser JS, Franz WB, 3rd. Neuroblastoma. *Am Fam Physician*. 1990;41(1):238-44.
4. Louis CU, Shohet JM. Neuroblastoma: Molecular Pathogenesis and Therapy. *Annu Rev Med*. 2015;66:49-63.
5. Betters E, Liu Y, Kjaeldgaard A, Sundstrom E, Garcia-Castro MI. Analysis of early human neural crest development. *Dev Biol*. 2010;344(2):578-92.
6. Thiery JP. Epithelial-mesenchymal transitions in tumour progression. *Nat Rev Cancer*. 2002;2(6):442-54.
7. Strobl-Mazzulla PH, Bronner ME. Epithelial to mesenchymal transition: new and old insights from the classical neural crest model. *Semin Cancer Biol*. 2012;22(5-6):411-6.
8. Pegoraro C, Monsoro-Burq AH. Signaling and transcriptional regulation in neural crest specification and migration: lessons from xenopus embryos. *Wiley Interdiscip Rev Dev Biol*. 2013;2(2):247-59.
9. Shtukmaster S, Schier MC, Huber K, Krispin S, Kalcheim C, Unsicker K. Sympathetic neurons and chromaffin cells share a common progenitor in the neural crest in vivo. *Neural Dev*. 2013;8:12.
10. Pugh TJ, Morozova O, Attiyeh EF, Asgharzadeh S, Wei JS, Auclair D, et al. The genetic landscape of high-risk neuroblastoma. *Nat Genet*. 2013;45(3):279-84.
11. Westermann F, Schwab M. Genetic parameters of neuroblastomas. *Cancer Lett*. 2002;184(2):127-47.
12. Guo C, White PS, Hogarty MD, Brodeur GM, Gerbing R, Stram DO, et al. Deletion of 11q23 is a frequent event in the evolution of MYCN single-copy high-risk neuroblastomas. *Med Pediatr Oncol*. 2000;35(6):544-6.
13. Attiyeh EF, London WB, Mosse YP, Wang Q, Winter C, Khazi D, et al. Chromosome 1p and 11q deletions and outcome in neuroblastoma. *N Engl J Med*. 2005;353(21):2243-53.
14. Srivatsan ES, Ying KL, Seeger RC. Deletion of chromosome 11 and of 14q sequences in neuroblastoma. *Genes Chromosomes Cancer*. 1993;7(1):32-7.
15. Fujita T, Igarashi J, Okawa ER, Gotoh T, Manne J, Kolla V, et al. CHD5, a tumor suppressor gene deleted from 1p36.31 in neuroblastomas. *J Natl Cancer Inst*. 2008;100(13):940-9.
16. Theissen J, Oberthuer A, Hombach A, Volland R, Hertwig F, Fischer M, et al. Chromosome 17/17q gain and unaltered profiles in high resolution array-CGH are prognostically informative in neuroblastoma. *Genes Chromosomes Cancer*. 2014;53(8):639-49.
17. Mullassery D, Dominici C, Jesudason EC, McDowell HP, Losty PD. Neuroblastoma: contemporary management. *Arch Dis Child Educ Pract Ed*. 2009;94(6):177-85.
18. Brodeur GM, Seeger RC, Schwab M, Varmus HE, Bishop JM. Amplification of N-myc in untreated human neuroblastomas correlates with advanced disease stage. *Science*. 1984;224(4653):1121-4.
19. Seeger RC, Brodeur GM, Sather H, Dalton A, Siegel SE, Wong KY, et al. Association of multiple copies of the N-myc oncogene with rapid progression of neuroblastomas. *N Engl J Med*. 1985;313(18):1111-6.
20. Huang M, Weiss WA. Neuroblastoma and MYCN. *Cold Spring Harb Perspect Med*. 2013.
21. Ardini E, Magnaghi P, Orsini P, Galvani A, Menichincheri M. Anaplastic Lymphoma Kinase: role in specific tumours, and development of small molecule inhibitors for cancer therapy. *Cancer Lett*. 2010;299(2):81-94.

The Effects of Hypoxic Preconditioning on the Oxygenation and Metabolic Profile of Neuroblastoma – Yousef Al-Mutawa

22. Shimada H, Ambros IM, Dehner LP, Hata J, Joshi VV, Roald B, et al. The International Neuroblastoma Pathology Classification (the Shimada system). *Cancer*. 1999;86(2):364-72.
23. Brodeur GM, Seeger RC, Barrett A, Berthold F, Castleberry RP, D'Angio G, et al. International criteria for diagnosis, staging, and response to treatment in patients with neuroblastoma. *J Clin Oncol*. 1988;6(12):1874-81.
24. Brodeur GM, Pritchard J, Berthold F, Carlsen NL, Castel V, Castelberry RP, et al. Revisions of the international criteria for neuroblastoma diagnosis, staging, and response to treatment. *J Clin Oncol*. 1993;11(8):1466-77.
25. Monclair T, Brodeur GM, Ambros PF, Brisse HJ, Cecchetto G, Holmes K, et al. The International Neuroblastoma Risk Group (INRG) staging system: an INRG Task Force report. *J Clin Oncol*. 2009;27(2):298-303.
26. Cohn SL, Pearson ADJ, London WB, Monclair T, Ambros PF, Brodeur GM, et al. The International Neuroblastoma Risk Group (INRG) Classification System: An INRG Task Force Report. <http://dxdoi.org/10.1200/JCO2008166785>. 2016.
27. Challis GB, Stam HJ. The spontaneous regression of cancer. A review of cases from 1900 to 1987. *Acta Oncol*. 1990;29(5):545-50.
28. Everson TC. Spontaneous regression of cancer. *Ann N Y Acad Sci*. 1964;114(2):721-35.
29. Papac RJ. Spontaneous regression of cancer: possible mechanisms. *In Vivo*. 1998;12(6):571-8.
30. Brodeur GM, Bagatell R. Mechanisms of neuroblastoma regression. *Nat Rev Clin Oncol*. 2014;11(12):704-13.
31. Yamamoto K, Ohta S, Ito E, Hayashi Y, Asami T, Mabuchi O, et al. Marginal decrease in mortality and marked increase in incidence as a result of neuroblastoma screening at 6 months of age: cohort study in seven prefectures in Japan. *J Clin Oncol*. 2002;20(5):1209-14.
32. Sawada T, Sugimoto T, Kawakatsu H, Matsumura T, Matsuda Y. Mass screening for neuroblastoma in Japan. *Pediatr Hematol Oncol*. 1991;8(2):93-109.
33. Erttmann R, Tafese T, Berthold F, Kerbl R, Mann J, Parker L, et al. 10 years' neuroblastoma screening in Europe: preliminary results of a clinical and biological review from the Study Group for Evaluation of Neuroblastoma Screening in Europe (SENSE). *Eur J Cancer*. 1998;34(9):1391-7.
34. Woods WG, Tuchman M, Robison LL, Bernstein M, Leclerc JM, Brisson LC, et al. A population-based study of the usefulness of screening for neuroblastoma. *Lancet*. 1996;348(9043):1682-7.
35. Schilling FH, Spix C, Berthold F, Erttmann R, Fehse N, Hero B, et al. Neuroblastoma screening at one year of age. *N Engl J Med*. 2002;346(14):1047-53.
36. Kerbl R, Urban CE, Ambros IM, Dornbusch HJ, Schwinger W, Lackner H, et al. Neuroblastoma mass screening in late infancy: insights into the biology of neuroblastic tumors. *J Clin Oncol*. 2003;21(22):4228-34.
37. DuBois SG, Kalika Y, Lukens JN, Brodeur GM, Seeger RC, Atkinson JB, et al. Metastatic sites in stage IV and IVS neuroblastoma correlate with age, tumor biology, and survival. *J Pediatr Hematol Oncol*. 1999;21(3):181-9.
38. Musarella MA, Department of Pediatric Ophthalmology THfSC, Toronto, Canada, Chan HSL, Department of Pediatric Hematology and Oncology THfSC, Toronto, Canada, DeBoer G, Ontario Cancer Institute T, Canada, et al. Ocular Involvement in Neuroblastoma: Prognostic Implications. *Ophthalmology*. 1984;91(8):936-40.
39. Hildebrandt T, Traunecker H. Neuroblastoma: A tumour with many faces. *Current Paediatrics*. 15(5):412-20.
40. David R, Lamki N, Fan S, Singleton EB, Eftekhari F, Shirkhoda A, et al. The many faces of neuroblastoma. *Radiographics*. 1989;9(5):859-82.
41. Kapoor PG, Chhabra R. Neuroblastoma presenting as raccoon eyes. *J Pediatr*. 2014;164(6):1495.

The Effects of Hypoxic Preconditioning on the Oxygenation and Metabolic Profile of Neuroblastoma – Yousef Al-Mutawa

42. Hanahan D, Weinberg RA. Hallmarks of cancer: the next generation. *Cell*. 2011;144(5):646-74.
43. Warburg O. On the Origin of Cancer Cells. 1956.
44. Brand RA. Biographical sketch: Otto Heinrich Warburg, PhD, MD. *Clin Orthop Relat Res*. 2010;468(11):2831-2.
45. Cairns RA, Harris IS, Mak TW. Regulation of cancer cell metabolism. *Nat Rev Cancer*. 2011;11(2):85-95.
46. Mazurek S, Boschek CB, Hugo F, Eigenbrodt E. Pyruvate kinase type M2 and its role in tumor growth and spreading. *Semin Cancer Biol*. 2005;15(4):300-8.
47. Yan H, Parsons DW, Jin G, McLendon R, Rasheed BA, Yuan W, et al. IDH1 and IDH2 mutations in gliomas. *N Engl J Med*. 2009;360(8):765-73.
48. Wise DR, DeBerardinis RJ, Mancuso A, Sayed N, Zhang XY, Pfeiffer HK, et al. Myc regulates a transcriptional program that stimulates mitochondrial glutaminolysis and leads to glutamine addiction. *Proc Natl Acad Sci U S A*. 2008;105(48):18782-7.
49. Vander Heiden MG, Cantley LC, Thompson CB. Understanding the Warburg Effect: The Metabolic Requirements of Cell Proliferation. *Science*. 2009;324(5930):1029-33.
50. Griffin JL, Shockcor JP. Metabolic profiles of cancer cells. *Nat Rev Cancer*. 2004;4(7):551-61.
51. Holmes E, Wilson ID, Nicholson JK. Metabolic phenotyping in health and disease. *Cell*. 2008;134(5):714-7.
52. Spratlin JL, Serkova NJ, Eckhardt SG. Clinical applications of metabolomics in oncology: a review. *Clin Cancer Res*. 2009;15(2):431-40.
53. Ryan D, Robards K. Metabolomics: The greatest omics of them all? *Anal Chem*. 2006;78(23):7954-8.
54. Patel S, Ahmed S. Emerging field of metabolomics: big promise for cancer biomarker identification and drug discovery. *J Pharm Biomed Anal*. 2015;107:63-74.
55. Emwas AH. The strengths and weaknesses of NMR spectroscopy and mass spectrometry with particular focus on metabolomics research. *Methods Mol Biol*. 2015;1277:161-93.
56. Emwas A-HM, Salek RM, Griffin JL, Merzaban JS, Advanced Nanofabrication IacCL, Division BaESaEB, et al. NMR-based metabolomics in human disease diagnosis: Applications, limitations, and recommendations. 2013.
57. Madu CO, Lu Y. Novel diagnostic biomarkers for prostate cancer. *J Cancer*. 2010;1:150-77.
58. Imperiale A, Elbayed K, Moussallieh FM, Neuville A, Piotta M, Bellocq JP, et al. Metabolomic pattern of childhood neuroblastoma obtained by ¹H-high-resolution magic angle spinning (HRMAS) NMR spectroscopy. *Pediatr Blood Cancer*. 2011;56(1):24-34.
59. Simon MC, Keith B. The role of oxygen availability in embryonic development and stem cell function. *Nat Rev Mol Cell Biol*. 2008;9(4):285-96.
60. Liu L, Ning X, Sun L, Zhang H, Shi Y, Guo C, et al. Hypoxia-inducible factor-1 alpha contributes to hypoxia-induced chemoresistance in gastric cancer. *Cancer Sci*. 2008;99(1):121-8.
61. Nardinocchi L, Puca R, Sacchi A, Rechavi G, Givol D, D'Orazi G. Targeting hypoxia in cancer cells by restoring homeodomain interacting protein-kinase 2 and p53 activity and suppressing HIF-1alpha. *PLoS One*. 2009;4(8):e6819.
62. Nordmark M, Alsner J, Keller J, Nielsen OS, Jensen OM, Horsman MR, et al. Hypoxia in human soft tissue sarcomas: adverse impact on survival and no association with p53 mutations. *Br J Cancer*. 2001;84(8):1070-5.
63. Durand RE. Keynote address: the influence of microenvironmental factors on the activity of radiation and drugs. *Int J Radiat Oncol Biol Phys*. 1991;20(2):253-8.
64. Brown JM, Wilson WR. Exploiting tumour hypoxia in cancer treatment. *Nat Rev Cancer*. 2004;4(6):437-47.
65. Ruan K, Song G, Ouyang G. Role of hypoxia in the hallmarks of human cancer. *J Cell Biochem*. 2009;107(6):1053-62.
66. Semenza GL. Targeting HIF-1 for cancer therapy. *Nat Rev Cancer*. 2003;3(10):721-32.

The Effects of Hypoxic Preconditioning on the Oxygenation and Metabolic Profile of Neuroblastoma – Yousef Al-Mutawa

67. Wang GL, Semenza GL. Characterization of hypoxia-inducible factor 1 and regulation of DNA binding activity by hypoxia. *J Biol Chem.* 1993;268(29):21513-8.
68. Forsythe JA, Jiang BH, Iyer NV, Agani F, Leung SW, Koos RD, et al. Activation of vascular endothelial growth factor gene transcription by hypoxia-inducible factor 1. *Mol Cell Biol.* 1996;16(9):4604-13.
69. Chen C, Pore N, Behrooz A, Ismail-Beigi F, Maity A. Regulation of glut1 mRNA by hypoxia-inducible factor-1. Interaction between H-ras and hypoxia. *J Biol Chem.* 2001;276(12):9519-25.
70. Fukuda R, Zhang H, Kim JW, Shimoda L, Dang CV, Semenza GL. HIF-1 regulates cytochrome oxidase subunits to optimize efficiency of respiration in hypoxic cells. *Cell.* 2007;129(1):111-22.
71. Carmeliet P, Dor Y, Herbert JM, Fukumura D, Brusselmans K, Dewerchin M, et al. Role of HIF-1alpha in hypoxia-mediated apoptosis, cell proliferation and tumour angiogenesis. *Nature.* 1998;394(6692):485-90.
72. Leuenroth SJ, Grutkoski PS, Ayala A, Simms HH. Suppression of PMN apoptosis by hypoxia is dependent on Mcl-1 and MAPK activity. *Surgery.* 2000;128(2):171-7.
73. Wolfe BB, Voelkel NF. Effects of hypoxia on atrial muscarinic cholinergic receptors and cardiac parasympathetic responsiveness. *Biochem Pharmacol.* 1983;32(13):1999-2002.
74. Mukhopadhyay CK, Mazumder B, Fox PL. Role of hypoxia-inducible factor-1 in transcriptional activation of ceruloplasmin by iron deficiency. *J Biol Chem.* 2000;275(28):21048-54.
75. Blouw B, Song H, Tihan T, Bosze J, Ferrara N, Gerber HP, et al. The hypoxic response of tumors is dependent on their microenvironment. *Cancer Cell.* 2003;4(2):133-46.
76. Shimoda LA, Fallon M, Pisarcik S, Wang J, Semenza GL. HIF-1 regulates hypoxic induction of NHE1 expression and alkalinization of intracellular pH in pulmonary arterial myocytes. *Am J Physiol Lung Cell Mol Physiol.* 2006;291(5):L941-9.
77. Vaupel P, Schlenger K, Knoop C, Hockel M. Oxygenation of human tumors: evaluation of tissue oxygen distribution in breast cancers by computerized O₂ tension measurements. *Cancer Res.* 1991;51(12):3316-22.
78. Hockel M, Schlenger K, Knoop C, Vaupel P. Oxygenation of carcinomas of the uterine cervix: evaluation by computerized O₂ tension measurements. *Cancer Res.* 1991;51(22):6098-102.
79. Dewhirst MW, Cao Y, Moeller B. Cycling hypoxia and free radicals regulate angiogenesis and radiotherapy response. *Nat Rev Cancer.* 2008;8(6):425-37.
80. Magat J, Jordan BF, Cron GO, Gallez B. Noninvasive mapping of spontaneous fluctuations in tumor oxygenation using 19F MRI. *Med Phys.* 2010;37(10):5434-41.
81. Smith H, Board M, Pellagatti A, Turley H, Boulwood J, Callaghan R. The Effects of Severe Hypoxia on Glycolytic Flux and Enzyme Activity in a Model of Solid Tumors. *J Cell Biochem.* 2016;117(8):1890-901.
82. Wigerup C, Pahlman S, Bexell D. Therapeutic targeting of hypoxia and hypoxia-inducible factors in cancer. *Pharmacol Ther.* 2016;164:152-69.
83. Hussein D, Estlin EJ, Dive C, Makin GW. Chronic hypoxia promotes hypoxia-inducible factor-1alpha-dependent resistance to etoposide and vincristine in neuroblastoma cells. *Mol Cancer Ther.* 2006;5(9):2241-50.
84. Herrmann A, Rice M, Levy R, Pizer BL, Losty PD, Moss D, et al. Cellular memory of hypoxia elicits neuroblastoma metastasis and enables invasion by non-aggressive neighbouring cells. *Oncogenesis.* 2015;4:e138.
85. Fardin P, Barla A, Mosci S, Rosasco L, Verri A, Versteeg R, et al. A biology-driven approach identifies the hypoxia gene signature as a predictor of the outcome of neuroblastoma patients. *Mol Cancer.* 2010;9:185.
86. Murphy JB, Rous P. THE BEHAVIOR OF CHICKEN SARCOMA IMPLANTED IN THE DEVELOPING EMBRYO. *The Journal of Experimental Medicine.* 1912;15(2):119-32.
87. Ribatti D. The chick embryo chorioallantoic membrane as a model for tumor biology. *Experimental Cell Research.* 2014;328(2):314-24.

The Effects of Hypoxic Preconditioning on the Oxygenation and Metabolic Profile of Neuroblastoma – Yousef Al-Mutawa

88. SK-N-AS ATCC [®] CRL-2137[®], ^ç Homo sapiens brain; derived from me 2018 [Available from: <https://www.atcc.org/products/all/CRL-2137.aspx#history>].
89. Xia J, Institute of Parasitology MUSAdBQC, Department of Animal Science MUSAdBQC, Department of Microbiology and Immunology MUMQC, Wishart DS, Department of Computing Science UoAEAC, et al. Using MetaboAnalyst 3.0 for Comprehensive Metabolomics Data Analysis. 2016;14.0.1-0.91.
90. Jombart T, Devillard S, Balloux F. Discriminant analysis of principal components: a new method for the analysis of genetically structured populations. *BMC Genet.* 2010;11:94.
91. Bertout JA, Patel SA, Simon MC. The impact of O₂ availability on human cancer. *Nat Rev Cancer.* 2008;8(12):967-75.
92. Chaplin DJ, Durand RE, Olive PL. Acute hypoxia in tumors: implications for modifiers of radiation effects. *Int J Radiat Oncol Biol Phys.* 1986;12(8):1279-82.
93. Bayer C, Vaupel P. Acute versus chronic hypoxia in tumors: Controversial data concerning time frames and biological consequences. *Strahlenther Onkol.* 2012;188(7):616-27.
94. Brurberg KG, Skogmo HK, Graff BA, Olsen DR, Rofstad EK. Fluctuations in pO₂ in poorly and well-oxygenated spontaneous canine tumors before and during fractionated radiation therapy. *Radiother Oncol.* 2005;77(2):220-6.
95. Braun RD, Lanzen JL, Dewhirst MW. Fourier analysis of fluctuations of oxygen tension and blood flow in R3230Ac tumors and muscle in rats. *Am J Physiol.* 1999;277(2 Pt 2):H551-68.
96. Rampling R, Cruickshank G, Lewis AD, Fitzsimmons SA, Workman P. Direct measurement of pO₂ distribution and bioreductive enzymes in human malignant brain tumors. *Int J Radiat Oncol Biol Phys.* 1994;29(3):427-31.
97. Human Metabolome Database: Showing metabocard for Trehalose (HMDB0000975) 2017 [Available from: <http://www.hmdb.ca/metabolites/HMDB0000975#links>].
98. Human Metabolome Database: Showing metabocard for Glutathione (HMDB0000125) 2017 [Available from: <http://www.hmdb.ca/metabolites/HMDB0000125>].
99. Traverso N, Ricciarelli R, Nitti M, Marengo B, Furfaro AL, Pronzato MA, et al. Role of glutathione in cancer progression and chemoresistance. *Oxid Med Cell Longev.* 2013;2013:972913.
100. Kotze H. *Systems Biology of Chemotherapy in Hypoxia Environments: The University of Manchester, Manchester, UK; 2012.*
101. Jiang C, Cai H, Peng X, Zhang P, Wu X, Tian R. Targeted Imaging of Tumor-Associated Macrophages by Cyanine 7-Labeled Mannose in Xenograft Tumors. *Mol Imaging.* 2017;16.
102. Movahedi K, Schoonooghe S, Laoui D, Houbracken I, Waelput W, Breckpot K, et al. Nanobody-based targeting of the macrophage mannose receptor for effective in vivo imaging of tumor-associated macrophages. *Cancer Res.* 2012;72(16):4165-77.
103. Silva VL, Al-Jamal WT. Exploiting the cancer niche: Tumor-associated macrophages and hypoxia as promising synergistic targets for nano-based therapy. *J Control Release.* 2017;253:82-96.
104. Tsai I-L, Kuo T-C, Ho T-J, Harn Y-C, Wang S-Y, Fu W-M, et al. Metabolomic Dynamic Analysis of Hypoxia in MDA-MB-231 and the Comparison with Inferred Metabolites from Transcriptomics Data. *Cancers.* 2013;5(2):491-510.
105. Kucharzewska P, Christianson HC, Belting M. Global profiling of metabolic adaptation to hypoxic stress in human glioblastoma cells. *PLoS One.* 2015;10(1):e0116740.
106. Chan EC, Koh PK, Mal M, Cheah PY, Eu KW, Backshall A, et al. Metabolic profiling of human colorectal cancer using high-resolution magic angle spinning nuclear magnetic resonance (HR-MAS NMR) spectroscopy and gas chromatography mass spectrometry (GC/MS). *J Proteome Res.* 2009;8(1):352-61.
107. Asano K, Miyamoto I, Matsushita T, Murakami Y, Minoura S, Wagatsuma T, et al. Succinic acidemia: a new syndrome of organic acidemia associated with congenital lactic acidosis and decreased NADH-cytochrome c reductase activity. *Clin Chim Acta.* 1988;173(3):305-12.
108. Elpeleg ON, Hurvitz H. Succinic acidemia is not a new syndrome of organic acidemia. *Clin Chim Acta.* 1990;188(3):271-2.

The Effects of Hypoxic Preconditioning on the Oxygenation and Metabolic Profile of Neuroblastoma – Yousef Al-Mutawa

109. Online Mendelian Inheritance in Man (OMIM) [Internet]. 2016. Available from: <http://omim.org/entry/248600#clinicalManagement>.
110. Rodrigues LM, Uribe-Lewis S, Madhu B, Honess DJ, Stubbs M, Griffiths JR. The action of β -hydroxybutyrate on the growth, metabolism and global histone H3 acetylation of spontaneous mouse mammary tumours: evidence of a β -hydroxybutyrate paradox. *Cancer Metab.* 2017;5.
111. Bonuccelli G, Tsigos A, Whitaker-Menezes D, Pavlides S, Pestell RG, Chiavarina B, et al. Ketones and lactate “fuel” tumor growth and metastasis: Evidence that epithelial cancer cells use oxidative mitochondrial metabolism. *Cell Cycle.* 2010;9(17):3506-14.
112. Goveia J, Pircher A, Conradi LC, Kalucka J, Lagani V, Dewerchin M, et al. Meta-analysis of clinical metabolic profiling studies in cancer: challenges and opportunities. *EMBO Mol Med.* 2016.
113. Kelly AD, Breitkopf SB, Yuan M, Goldsmith J, Spentzos D, Asara JM. Metabolomic profiling from formalin-fixed, paraffin-embedded tumor tissue using targeted LC/MS/MS: application in sarcoma. *PLoS One.* 2011;6(10):e25357.